UNIVERSITAT POLITÈCNICA DE VALÈNCIA

Escola Tècnica Superior d'Enginyeria Agronòmica i del Medi Natural

Functional effects of the genetic manipulation of the phosphorylation state of the Target of Rapamycin effector Npr1

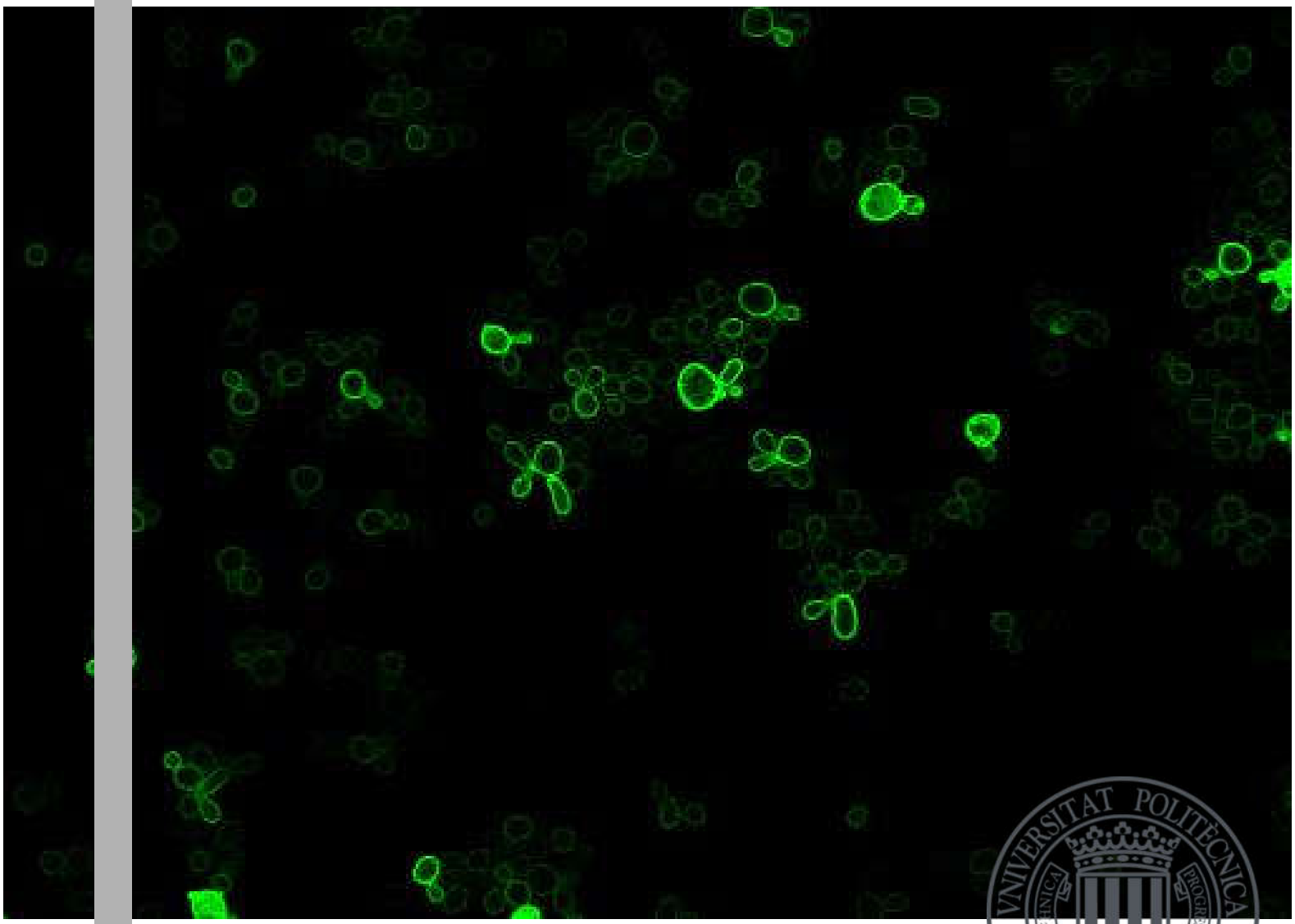

AUTHOR: CLARA ALBIÑANA CLIMENT

TUTOR: LYNNE YENUSH

2015/2016

BACHELOR'S DEGREE IN BIOTECHNOLOGY

VALÈNCIA, JULY 2016

SUMMARY

Title: Functional effects of the genetic manipulation of the phosphorylation state of the Target of Rapamycin effector Npr1.

Abstract: The behavior of microorganism is based on optimizing its growth and maximizing its survival. These cells are able to assess the quantity and quality of available nutrients and adjust their transcriptional, metabolic and developmental profiles accordingly to provide the proper set of proteins responsible for uptake, transport, and processing of the nutrients. The TORC1 (Target Of Rapamycin Complex 1) signaling pathway is a central controller of cell growth and is largely responsible for the coordination of the cellular response to changes in nitrogen source and availability. The flux of amino acids and other nitrogenous compounds transported into the cell depends on membrane protein transporters known as permeases. Opposing and parallel mechanisms of endocytosis of existing permeases and delivery of new ones determine the amount and collection of these proteins present in the PM at any given time. The endocytosis and subsequent degradation of these permeases is regulated by post-translational modifications in which ubiquitylation plays a fundamental role. Rsp5 is a HECT family E3 ubiquitin ligase in S. cerevisiae which is responsible for the ubiquitylation of the majority of nutrient and amino acid permeases. The interaction occurs via adaptor proteins, many of which belong to the ART family (arrestin-related trafficking). These adaptors determine the Rsp5 specificity for the membrane permeases. Npr1 is one of the targets of phosphorylation of TORC1 and promotes the activity of diverse transport systems for nitrogenous nutrients. It has been identified as the TORC1 effector kinase responsible for the signal transduction to the ARTs. More specifically, Npr1 has been shown to phosphoinhibit Art1 directly resulting in the inhibition of Rsp5-mediated endocytosis of permeases. Moreover, Npr1 is also able to bind to and phosphorylate Art3, although the consequences of this regulation have yet to be established. Npr1 activity is regulated through its phosphorylation state, being active when dephosphorylated and inactive when phosphorylated. In this project we attempted to further explore this particular TORC1-dependent regulatory mechanism of ART-mediated ubiquitylation and subsequent endocytosis of nutrient transporters by hypothesizing that the phosphorylation state of Npr1 correlates with its functionality in the context of this process. This hypothesis was explored by using different experimental approaches to analyze a set of mutant strains described to have a permanent effect on the phosphorylation state of Npr1.

Key words: Npr1, Target of Rapamycin Complex 1, amino acid transport, phosphorylation, arrestins, endocytosis, *Saccharomyces cerevisiae*

Títol: Efectes funcionals de la manipulació genética de l'estat de fosforilació de l'efector de Target Of Rapamycin (diana de rapamicina) Npr1.

Resum: El comportament dels microorganismes està basat en optimitzar el seu creixement i maximitzar la seua supervivència. Estes cèl•lules tenen la capacitat d'avaluar la quantitat i qualitat de nutrients disponibles i d'ajustar consegüentment els seus perfils transcripcionals, metabòlics i de desenvolupament per proporcionar el conjunt apropiat de les proteïnes responsables del consum, transport i processament dels nutrients. La ruta de senyalització TORC1 (Target Of Rapamycin Complex 1), o complex diana de la rapamicina, és un controlador central del creixement cel•lular i és en gran part responsable de la coordinació de la resposta cel•lular als canvis en la font i la disponibilitat del nitrogen. El flux d'aminoàcids i altres compostos nitrogenats transportats cap a l'interior cel•lular depèn d'uns transportadors de membrana anomenats permeases. Els mecanismes oposats i en paral•lel d'endocitosis de permeases existents i el lliurament de noves determinen la quantitat i diversitat d'estes proteïnes a la membrana plasmàtica en cada moment. L'endocitosi i subsegüent degradació d'estes permeases és regulat per modificacions post-traduccionals, on la ubiquitinació juga un paper fonamental. Rsp5 és una E3 ubiquitina ligasa de S. cerevisiae de la família HECT responsable de la ubiquitinació de la majoria de les permeases dels nutrients i aminoàcids. La interacció es dóna via proteïnes adaptadores, on moltes de les quals pertanyen a la família ART (arrestin-related trafficking) o proteïnes adaptadores de tràfic relacionades amb arrestina. Estos adaptadors determinen l'especificitat de Rsp5 per les permeases de membrana. Npr1 és una de les dianes de fosforilació de TORC1 i promou l'activitat de diversos sistemes de transport de nutrients nitrogenats. S'ha identificat com la quinasa efectora de TORC1 és responsable de la transducció del senyal a les ARTs. Específicament, s'ha demostrat que Npr1 fosfoinhibeix directament a Art1, el qual resulta en la inhibició de l'endocitosi de permeases mediada per Rsp5. A més, Npr1 també és capaç d'unir-se i fosforilar Art3, encara que les conseqüències d'aquesta regulació encara no s'han establert. L'activitat de Npr1 es regula a través del seu estat de fosforilació, estant actiu quan es troba desfosforilat i inactiu quan es troba fosforilat. En aquest projecte s'ha intentat arribar més lluny en l'exploració d'este particular mecanisme depenent de TORC1 d'ubiquitinació mediada per les ARTs i de la subsegüent endocitosi de transportadors de nutrients fent la hipòtesi on l'estat de fosforilació de Npr1 es correlaciona amb la seua funcionalitat en el context d'aquest procés. La hipòtesi va ser explorada utilitzant diferents plantejaments experimentals per a analitzar un conjunt de cepes mutants en les quals s'havia descrit un efecte permanent en l'estat de fosforilació de Npr1.

Paraules clau: Npr1, complex 1 de la diana de rapamicina, transport d'aminoàcids, fosforilació, arrestines, endocitosi, *Saccharomyces cerevisiae*

Author: Clara Albiñana Climent

Tutor: Dr. Lynne Yenush

València, July 2016

Thank you

No era partidària d'escriure uns agraïments com a tal per diverses raons però, ara que he acabat per fi, m'ha vingut la necessitat de deixar alguna cosa personal ací més que res per a que els involucrats sapigueu quant de sincerament agraïda estic (per si no ho he expressat en paraules ja) i probablement també per a poder rellegir-ho jo, que ho sé massa.

Estos mesos han representat una època molt important per a mi i, sincerament, no haguera predit mai tot el que he après fent este treball, en tots els aspectes.

Està de més agrair a Alba i a Coté perquè se'ns ha notat de sobra lo a gust que hem estat juntes. I tampoc puc oblidar-me de Ceci, a la que li dec la major part de coses que he après.

Tengo muchísimo que agradecer a Lynne. Te ha costado confiar y por eso me he esforzado mucho más. Y, al final, he podido llegar al punto de sentirme orgullosa de algo que yo haya hecho. Y eso ha pasado tanto con tu asignatura como con este proyecto. Me siento realmente honrada de haber podido trabajar aquí.

I, encara que vullga, no puc obviar a Alejandro Mossi. Ningú pot obviar a Alejandro Mossi, és una persona massa brillant. Res haguera sigut igual sense tu.

Per últim done les gràcies al sempre incondicional apoyo logístico i a Elisa, per baixar-me del núvol quan m'has dit sincerament que no t'interessava ni lo més mínim el que t'estava contant.

CLARA

INDEX

INDEX FIGURES AND TABLES

FIGURES

Introduction

Results

Discussion

Annex

TABLES

Materials & Methods

ABBREVIATIONS

AzC	L-Azetidine-2-carboxylic acid
CAN1	CANavanine resistance. Arginine permease
DMSO	Dimetil Sulfóxido
ER	Endoplasmic reticulum
EDTA	Ethyldiaminotetraacetic acid
END	Endocytic pathway
GAP1	General amino acid permease
GFP	Green fluorescent protein
HA	Hemagglutinine
HECT	Homologus to E6-AP C-Terminus
LB	Luria Bertani medium
MVP	Multivesicular body
Npr1	Nitrogen permease reactivator
OD	Optical density
PEG	Polyethyleneglycol
PI3P	Phosphatidylinositol 3-phosphate
PM	Plasma membrane
PY	Amino acid motif containing PPxY
RAP	Rapamycin
RING	Really interesting new gene
SD	Synthetic drop-out
SDS	Sodium dodecyl sulphate
SDS-PAGE	Sodium dodecyl sulphate polyacrylamide gel electrophoresis
SEC	Secretory pathway
TBS	Tris-Buffered-Saline
TCA	Trichloroacetic acid
TOR	Target of rapamycin
TORC1	Target of rapamycin complex 1
TORC2	Target of rapamycin complex 1
Ub	Ubiquitin
VAC	Vacuole
WT	Wild type
YNB	Yeast nitrogen base
YPD	Yeast extract-peptone-dextrose

Introduction

1. Nutrient Transport and Cell Growth in the model organism *Saccharomyces cerevisiae*

Like many other unicellular microorganism, *S. cerevisiae* behaves in a way that optimizes its growth and maximizes its survival (Zaman et al. 2008). "Growth is not simply an accumulation of mass. It is a carefully orchestrated accumulation of mass, occurring only at specific times and places" (Schmelzle and Hall 2000). Yeast cells are able to assess the quantity and quality of available nutrients and adjust their transcriptional, metabolic and developmental profiles accordingly to provide the proper set of proteins responsible for uptake, transport, and processing of the nutrients.

As all eukaryotic cells, they have a wide range of membrane integral proteins whose function is to ensure correct nutrient transport (Van Belle and André 2001). The coordination between nutrient uptake (building blocks) and nutritional requirements is important, so that the growth rate is proportional. Numerous signal transduction pathways mediate this behavior.

To ensure their own survival, yeast carry out a hierarchical consumption of available nutrients, with an order of preference for the different carbon and nitrogen sources in the medium (De Virgilio and Loewith 2006). This characteristic is based on the cell's ability to dynamically remodel the transport proteins present in the plasma membrane (PM), presenting the optimal nutrient transporters for the specific environment. Endocytic downregulation is a key mechanism for the control of protein composition and organization of the PM. The intracellular trafficking of these proteins is typically controlled according to substrate availability, general nutrient supply and/or stress conditions (Lauwers et al. 2010).

1.1. Plasma membrane transporters

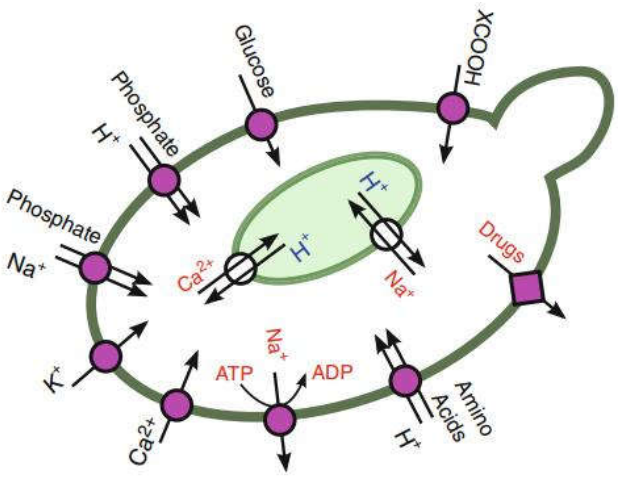

Figure 1.1: Scheme of the yeast membrane transporters. A schematic picture of a yeast cell with several organelles and fluxes of different important substrates. (Kschischo, Ramos and Sychrová 2016).

As the plasma membrane only allows water and small lipophilic molecules to permeate by simple diffusion through its structure, transmembrane transport proteins play a crucial role in all cells – from unicellular organism to mammals- by conferring to plasma and internal membranes selective permeability to a wide range of molecules such as ions, sugars, amino acids, nucleotides, and many other cell metabolites (Lauwers et al. 2010).

The number of proteins with membrane transport function (predicted or established) in *S. cerevisiae* stands at around 320 (Van Belle and André 2001), which represents 6% of the

whole proteome, including the intracellular transporters in the mitochondria and vacuole. In Figure 1.1, an overall view of these membrane transporters and their major substrates is depicted.

In yeast, membrane transporters play crucial roles in very diverse functions such as nutrient uptake, drug resistance, salt tolerance, control of cell volume, efflux of undesirable metabolites and sensing of extracellular nutrients. They are generally classified in three main categories: channels, permeases (also called *facilitators*, *transporters, carriers*), and pumps (Andre 1995). Pumps consist of active primary transport systems, generating electrochemical ion gradients from light or chemical energy and, therefore, creating cross-membrane potentials. We can find two types of pumps: PM ATPases and ABC transporters. Facilitators consist of active secondary transport systems, where the energy for translocation of one solute is supplied by an electrochemical gradients of another solute, generally created by a pump (van der Rest et al. 1995). The three general categories of secondary transport systems are uniport, symport and antiport. Uniport systems facilitate the transport of a single solute down its concentration gradient. The best-known examples of electroneutral uniport in S. cerevisiae are the transporters for the monosaccharides glucose and galactose (HXT1-7, GAL2). Symport systems involve the coupled movement of two or more solutes in the same direction, making use of one's gradient to transport the others. In yeast, most ions and disaccharides are coupled to proton symport systems, whereas this system is the only one for amino acid transport as well as for the nucleosides cytosine and uracil (van der Rest et al. 1995). Finally, antiport systems couple the movement of various cations and protons in opposite directions though the PM.

1.1.1. *Nitrogen permeases*

Each of the major nutrient types has a series of particular transporters (Van Belle and André 2001). In this particular project the focus will be on the transporters used for the intake of nitrogen compounds, specifically amino acids and nucleosides.

In yeast, amino acid transport has been attributed to 18 proteins of the same family (AAP, amino acid permeases), relying exclusively on proton-coupled symport (van der Rest et al. 1995). These transporters are classified according to substrate specificity into two main groups: high-affinity permeases and broad-affinity permeases. Most of the permeases are highly specific for particular amino acids (arginine permease Can1, proline permease Put4 and histidine permease Hip1) or various (Tat1 permease has high-affinity for tyrosine, isoleucine, valine, histidine, tryptophan and cysteine), whereas the general amino acid permease Gap1 has low-affinity for all of them. This is also true for nucleoside transporters, having a broad specificity transporter, Fey2, with affinity for adenine, guanine, hypoxantine and cytosine (Polak and Grenson 1973) and a high-affinity transporer of uracil, Fur4 (Jund, Weber and Chevallier 1988).

Yeast can use a wide variety of compounds as carbon or nitrogen sources. However, when provided with a mixture, they exclusivly use preferred carbon and nitrogen sources before non-preferred, suboptimal ones (De Virgilio and Loewith 2006). In the case of a preferred nitrogen source such as glutamate, the function of the permeases is to transport amino acids for their use in protein synthesis, so high-specificity permeases provide more control of this process. During growth on poor nitrogen sources, such as proline or urea, amino acid uptake serves as a nitogen source, so the high specificty of the permeases is not required and so are replaced with low affinity, high capacity transporters, such as Gap1 (Merhi and André 2012).

2. Regulation of the plasma membrane transporters

As referred to above, yeast cells subtly tune their growth in accordance with the nature and availability of nutrients in a manner that maximizes survival. When a change is perceived, they actively adjust their transcriptional, metabolic and biosynthetic capabilities to match that perception (Broach 2012). There are diverse signaling routes that integrate extracellular signals with cellular response, in which the *Target of Rapamycin* (TOR) pathway plays a central role (this complex will be more extensively explained in a following section).

Consequently, membrane transport proteins are regulated at three levels: gene transcription, intracellular membrane trafficking of the synthesized proteins and modulation of intrinsic activity. The most recent research has highlighted the importance of the different membrane transporters traffic pathways, summarized below in Figure 1.2.

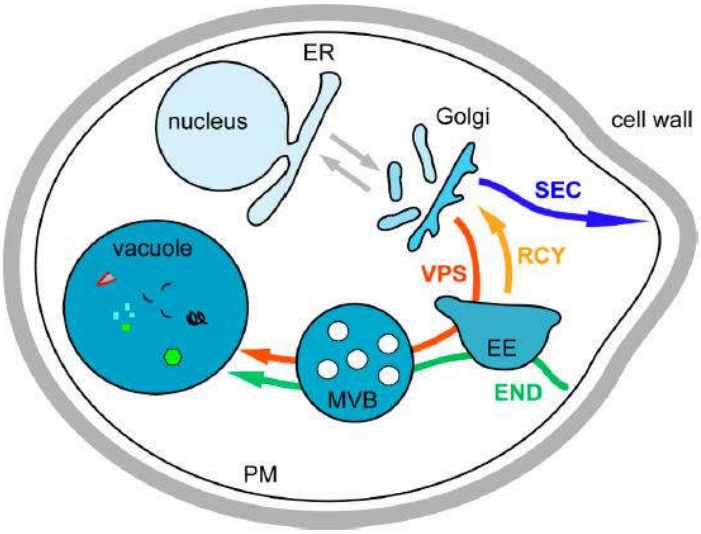

Figure 1.2: Representation of the different yeast intracellular trafficking pathways. Both secretion and membrane proteins (PM and organelles) are synthesized in the endoplasmic reticulum (ER) and transported to the Golgi (grey arrow) where they are sorted into vesicles through the trafficking network. These vesicles can join the secretory (SEC) pathway, for plasma membrane and extracellular proteins (blue arrow), or can be sorted into vacuolar protein sorting (VPS) vesicles for vacuolar proteins passing through endosomes (red arrow). The endocytic pathway (END) is used for internalization of PM proteins (green arrow). At the early endosomes (EE), proteins are sorted between those targeted for degradation into the vacuole through the multivesicular body (MVB) and those following the recycling pathway (RCY). (Feyder et al. 2015).

Most of the trafficking effectors, complexes and pathways involved in the processes of PM remodeling and membrane trafficking were identified by studies in *S. cerevisiae*, and are very well conserved among eukaryotes (Conibear 2010). At least three levels of trafficking control have been described to date. The first level involves the endocytosis and endosome/vacuole degradation of the internalized protein. The second, the possibility of the deviation of the PM targeted newly synthesized transporters to the vacuole. The third level implies the storage of some transporters in intracellular membranes in order to recycle them in response to specific signals (Haguenauer-Tsapis and André 2004). Although these control mechanisms happen simultaneously, a large number of studies have focused on the removal of proteins in response to environmental cues, or endocytic downregulation. This project will focus on this level of control of the PM transporters.

2.1. Endocytic downregulation of PM transporters

The yeast endocytic pathway (END) takes part in the regulation of the protein composition of the PM. When there is a change in the environmental conditions, endocytosis is required to eliminate membrane permeases whose specific molecules are no longer necessary or could be harmful to the cell.

PM proteins (also called *cargos*) and extracellular medium are internalized to the cell interior and subsequently transported through early endosomes and late endosomes (also known as Multi-Vesicular Bodies, MVB) before reaching either the vacuole/lysosome for degradation or transport back to the TGN for recycling (Conibear 2010), as represented in green and yellow arrows in Figure 1.2. The stability of integral proteins in the PM is highly controlled by post-translational modifications. This process is more extensively described in the following section, but it is important to highlight the importance of the ubiquitin polypeptide to target PM proteins for their internalization and consequent entrance into the endocytic pathway (Hicke 1997).

The ABC-transporter Ste6 (Kölling and Hollenberg 1994) and the multidrug transporter Pdr5 (Egner and Kuchler 1996) are examples of the many membrane transporters for which ubiquitylation is essential for their endocytosis. Indeed, the general consensus is that ubiquitin-mediated endocytosis is the dominant mechanism for internalization of most cargoes studied in yeast (MacGurn, Hsu and Emr 2012).

3. The Ubiquitin signal in cellular traffic

3.1. Ubiquitin Conjugation

Ubiquitin (Ub) is a highly conserved 76 amino acid polypeptide that acts as a post-translational modification through covalent conjugation to diverse target proteins. Its conjugation process is referred to as ubiquitylation and results in the formation of an isopeptide bond between the C-terminal glycine of the ubiquitin molecule and free amino groups on lysine side chains or to the N-terminal amino group of a target protein. This reaction requires the sequential and cooperative actions of three classes of enzymes (Ravid and Hochstrasser 2008): a ubiquitin-activating enzyme (E1), a ubiquitin-conjugating enzyme (E2) and a ubiquitin ligase (E3).

The ubiquitylation process is well-defined and highly conserved among eukaryotes (Figure 1.3). Ubiquitin is first activated by an E1 activating enzyme through the creation of a thioester bond between its C-terminus and a cysteine residue on the active site of the enzyme. Next, the activated ubiquitin is transferred and conjugated to an E2 conjugating enzyme through the same mechanism. The final step, catalyzed by an E3 ligase, consists of transferring the Ub to an acceptor lysine in the substrate protein. This process is carried out differently by each family of E3 ligases (see the following section).

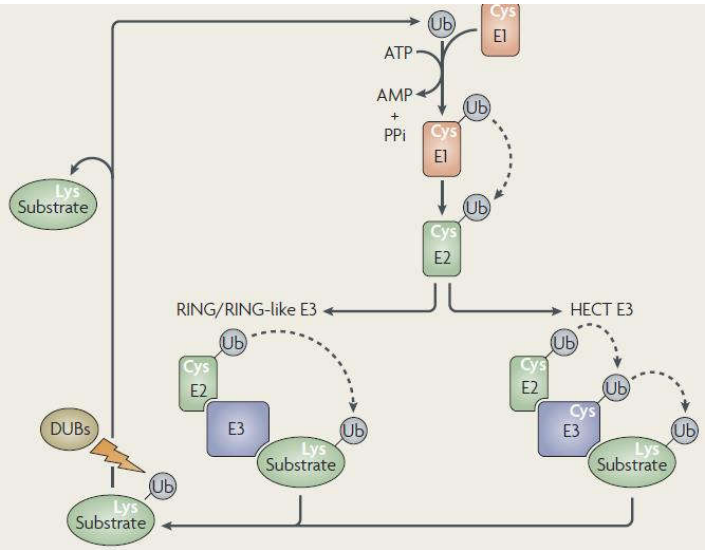

Figure 1.3: Ubiquitin conjugation. Ubiquitylation involves the concerted activities of the 3-enzyme system. The E1 covalently binds a Ub in an ATP-dependent manner, the E2 receives the Ub from the E1 and physically assembles with an E3. The E3 in turn binds substrate proteins and facilitates the transfer of the Ub to the bound substrate. In the case of the RING family, the Ub is passed directly from the E2 to the target protein, whereas the HECT family E3 ligases participate in the transfer process. Deubiquitylation is catalyzed by DUBs. (Ravid and Hochstrasser 2008).

The organization of the enzymatic conjugating cascade is hierarchical: There is only one E1 gene in yeast, while there are 11 E2 enzymes and 54 E3 ligases, with increasing variety in higher eukaryotes (Hicke, Schubert and Hill 2005). Each E3 recognizes a set of substrates that share one or more ubiquitylation signals, and cooperates with one or a few E2s (Pickart 2001).

Ubiquitylation is reversible, the activity of ubiquitin ligases can be antagonized by a series of deubiquitinating enzymes or DUBs (Komander, Clague and Urbé 2009). These DUBs are selective for different classes of ubiquitin chain substrates, adding an extra level of control to the process. They are also fundamental for maintaining a balanced level of free ubiquitin molecules.

3.2. E3 ubiquitin ligases

The E3 reaction involves at least two distinct steps: E3 binding to the substrate via the ubiquitylation signal, and the covalent ligation of one or more ubiquitin moieties to the substrate.

The known E3 enzymes are members of two protein superfamilies: RING E3s and HECT domain E3s, being their catalytic modules unrelated in sequence or structure. However, they share the E2-binding capacity. The RING (Really Interesting New Gene) and RING-like superfamily covers the majority of E3 ligases. They mediate the direct transfer of the ubiquitin from the E2 to the substrate by bringing both elements into proximity. The HECT (Homologous to E6AP Carboxyl Terminus) domain superfamily enzymes, on the other hand, contain a catalytic cysteine residue in their HECT domain capable of accepting the ubiquitin themselves, before transferring it to the substrate (Metzger, Hristova and Weissman 2012).

3.3. Ubiquitylation of PM proteins

Although first identified as a modification in cytosolic proteins for proteosomal degradation, this is not the only fate possible for ubiquitin-tagged proteins. Besides promoting the internalization of PM proteins, as stated above, ubiquitin is also important for cargo classification in membrane trafficking (Katzmann, Odorizzi and Emr 2002), as well as many other critical cellular functions. Ubiquitylation is further diversified by the generation of poly ubiquitin chains of different structures, which are assembled through bonds between the C-terminal glycine and any of its seven lysine residues or N-terminus. Alternatively, the amino terminus can be used to extend ubiquitin chains. The range of structures determines the different functions (Komander 2009), the K48 and K63 modifications are the most extensively characterized. As for yeast permeases, the consensus is that ubiquitin-mediated membrane trafficking events in the cell are mainly directed by monoubiquitylation and K63-linked polyubiquitylation (Lauwers et al. 2010).

A HECT family E3 ubiquitin ligase, Rsp5, has been shown to be the key player in constitutive and regulated PM protein ubiquitylation, triggering their entry of the majority of plasma membrane proteins into the endocytic pathway (Rotin, Staub and Haguenauer-Tsapis 2000).

4. Rsp5 and the ARTs Adaptor Family

4.1. The Rsp5 E3 ubiquitin ligase

The Nedd4 family belongs to the HECT superfamily of E3 enzymes, the only known E3 enzymes that form ubiquitin-thioester intermediates and directly catalyze substrate ubiquitylation. Although nine

Nedd4 family members have been identified in the human genome, Rsp5 is the sole representative of this family in yeast. The Rsp5 ubiquitin ligase possesses three WW domains (Rotin et al. 2000) enabling it to interact with short consensus sequences P/LPXY (PY motifs) present in substrate proteins. Yet most yeast transporters under Rsp5 control do not possess such motifs. Actually, Rsp5 binds via its WW domain to PY motifs in accessory proteins acting as specific adaptors for cargo ubiquitylation (Lauwers et al. 2010). These proteins belong mostly to the arrestin-related trafficking (ART) adaptor family (Lin et al. 2008), but there are also adaptors from other families (Merhi and André 2012).

4.2.The Arrestin Related Trafficking (ART) Adaptor Family

4.2.1. ART structure

So far, 10 members of the ART family have been established in yeast as scaffold adaptors for Rsp5, accounting for the variety and specificity of its interaction (Lin et al. 2008) (Nikko, Sullivan and Pelham 2008). The ART proteins are characterized by a conserved structure, with N-terminal arrestin homology and several C-terminal PY motifs (Figure 1.4).

These proteins resemble a subclass of mammalian arrestin-like proteins, named arrestin domain-containing proteins (ARRDC) or α-arrestins, also containing PY motifs (Becuwe et al. 2012). The name is therefore due to structural and functional similarities, as these arrestins are also implicated in the endocytic downregulation of various PM proteins (Lefkowitz, Rajagopal and Whalen 2006).

While the ART-Rsp5 interaction is well characterized, the cargo binding interaction has not been described in detail, although all signs point to the arrestin domain being responsible for this union.

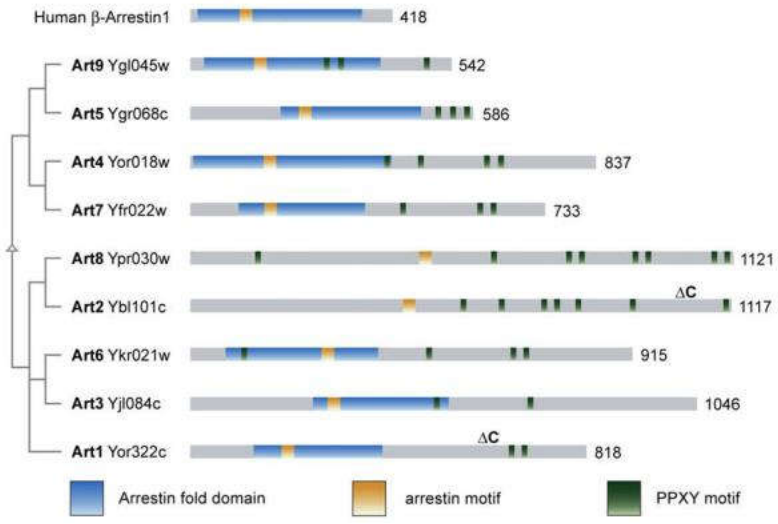

Figure 1.4. Schematic representation of the phylogenetic relationship of the ART adaptor family. Each member features the arrestin domain, homologous to the human β-arrestin and various N-terminus PY motifs. The systematic name of each gene is indicated, along with the ART nomenclature alias. (Lin et al. 2008).

4.2.2. ARTs as adaptors for PM protein ubiquitylation

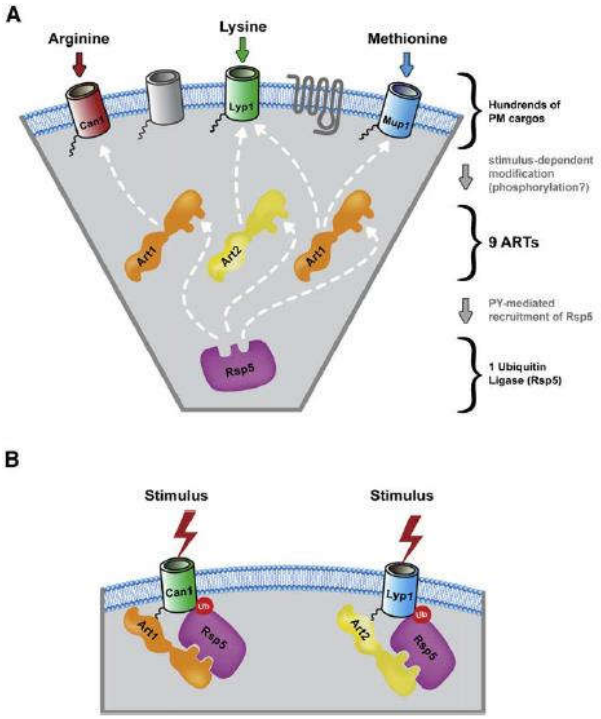

Figure 1.5. A model for ARTs as cargo-specific ubiquitin ligase adaptors. The abundance of integral PM proteins must be regulated in response to environmental stimuli (A) A variety of cargos require Rsp5-mediated ubiquitylation for their endocytic downregulation and, lacking the PY motifs needed for that interaction, make use of the cargo-specificity of the ART family proteins and use them as adaptors. (B) In response to specific stimuli, ART proteins recognize specific cargos in the PM and recruit the Rsp5 ubiquitin ligase. Ubiquitylation triggers endocytosis, traffic to the vacuole and degradation. (Lin et al 2008).

Although the ART family has been implicated in other cellular functions, such as in the mediation of Golgi-to-endosome traffic (O'Donnell et al. 2010), their principal functions is to mediate Rsp5 association to PM transporters. These interactions are necessary to lead Rsp5 to the PM (O'Donnell et al. 2010). In addition, the fact that Art1 is required for endocytosis of three permeases (Can1, Mup1 and Lyp1) but not several others (Fur4, Ftr1, Pdr5 and Ste2) confers a degree of specificity to this interactions (Polo and Di Fiore 2008).

The adaptor function of the ARTs was demonstrated by the requirement of Art1 for the endocytic downregulation of the arginine transporter Can1 and the methionine transporter Mup1, and of Art2 for the internalization of Lyp1, a lysine transporter (Figure 1.5) (Lin et al. 2008).

A proteome-wide analysis of phosphorylation in yeast demonstrated that ART family proteins are extensively phosphorylated in vivo (Albuquerque et al. 2008). Later on, it was found that extracellular cues induced these phosphorylation changes in some ART proteins, altering their trafficking and signaling activities (O'Donnell et al. 2010).A recent model identifies the Npr1 protein kinase as being responsible for the integration of the extracellular cues for the Rsp5-mediated endocytosis of Can1 through phosphorylation of Art1, upon inactivation of TORC1 (MacGurn et al. 2011). It is interesting to emphasize that this model for ARTs as cargo-specific Rsp5 adaptors is responsive to specific stimuli, such as nutrient availability and stress.

5. The TOR Signaling Pathway

5.1. The TOR protein kinase

TOR (Target Of Rapamycin) is a serine/threonine protein kinase highly conserved from yeast to mammals (Loewith and Hall 2011). Due to its homology with the phosphatidylinositol kinase (PIK) family it is classified in the PIK-related kinases family (PIKK), but it has no lipid kinase activity (Keith and Schreiber 1995).

All TORs share a similar domain structure. From C- to N-terminus: the FATC domain, the kinase domain, the FRB domain, the FAT domain and the so-called HEAT repeats (Figure 1.6A). There are about 20 HEAT motif repeats within the N-terminal half of TOR that function as a platform for the subunits of the TOR complexes (Kunz et al. 2000).

In addition to being originally characterized in *S. cerevisiae* (Kunz et al. 1993, Helliwell et al. 1994), this model organism is the only one known to have two TOR genes, TOR1 and TOR2.

5.2. Rapamycin

Rapamycin is a lipophilic macrolide and a natural secondary metabolite produced by *Streptomyces hygroscopicus* discovered for its antibiotic properties (Heitman, Movva and Hall 1991). Its mechanism of action is based on the inhibition of the TOR signaling pathway, hence the name: Target Of Rapamycin. The high-affinity union of rapamycin with FKBP12 (FK506-binding protein, encoded in yeast by the *FPR1* gene) allows this complex to bind to the FRB domain of the TOR kinase (Choi et al. 1996, Lorenz and Heitman 1995). Although it is not completely clear, the complex might inhibit the kinase activity of TOR either directly or by blocking its access to substrates or accessory proteins (Crespo and Hall 2002, Loewith and Hall 2011).

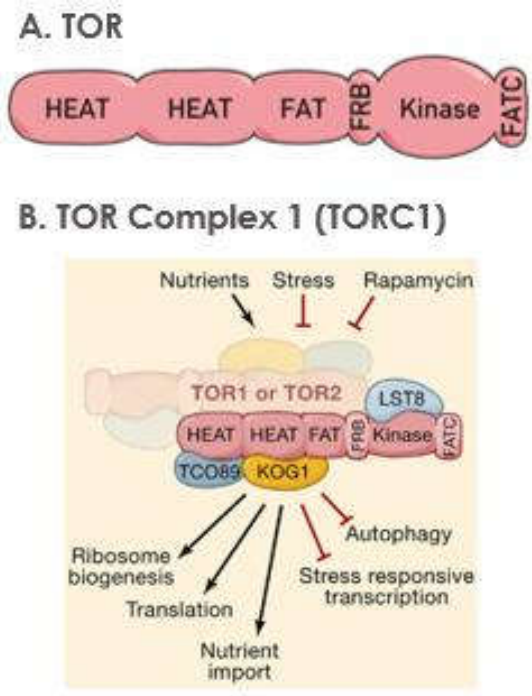

Figure 1.6. A. Conserved domain structure of TOR. From N- to C-terminus: two blocks of HEAT repeats, FAT domain (modified HEAT repeats), FRB (FKBP12-rapamycin-binding), kinase domain, FATC domain (essential for kinase activity). (Loewith and Hall 2011). **B. Structure and functions of TORC1.** The TOR complex 1 is composed of Tor1 or Tor2 and a set of accessory proteins: Tco89, Lst8 and Kog1. TOR1 regulates cell growth by adjusting the equilibrium between biosynthesis and turnover in a cell, in response to an integrated set of environmental cues. (Wullschleger, Loewith and Hall 2006).

The physiological effect of rapamycin is much the same as nutrient starvation (Barbet et al. 1996), and this was the first indicator of the role of TOR in the regulation of growth in response to nutrient cues.

5.3. Cellular functions of TOR in *S. cerevisiae*: TOR complexes

Although structurally similar, TOR1 and TOR2 are not functionally identical. As described, TOR2 has two essential functions in two separate signaling branches: one redundant with TOR1 and another unique (Hall 1996, Helliwell et al. 1998). Indeed, the TOR kinases function as components of two regulatory multiprotein complexes, TOR complex 1 (TORC1) and TOR complex 2 (TORC2), which control cell growth in different ways (Loewith et al. 2002).

TORC1 is the assembly of Kog1, Lst8, Tco89 and either TOR1 or TOR2. It controls cell growth via a rapamycin-sensitive signaling branch regulating translation, transcription, ribosome biogenesis, nutrient transport and utilization, autophagy and stress responses (Figure 1.6B). TORC2, on the other hand, is composed of different elements with TOR2 and it controls the organization of the actin

cytoskeleton and sphingolipid biosynthesis, among other functions, through a rapamycin-insensitive signaling branch (Wullschleger et al. 2005). This project focuses on the TORC1 signaling pathway and its integration of physiological conditions to cellular response.

5.4.TORC1 Signaling

TORC1 is the central controller of cell growth i.e. the balance between macromolecular biosynthesis and turnover. The complex responds to various cellular and environmental cues including nutrient availability, energy status, and growth signals. When the physiological conditions are optimum TORC1 promotes protein synthesis while, at the same time, antagonizes autophagy, represses the endogenous nutrient synthesis pathways and inhibits stress responses (Wei and Zheng 2011). TORC1 positively controls protein synthesis at multiple levels. A particularly relevant indirect control mechanism involves the activity of high-affinity amino acid permeases that mediate amino acid uptake for immediate use by the translation machinery (De Virgilio and Loewith 2006). This pathway, involving the Rsp5 E3 ubiquitin ligase, will be discussed further below.

As observed, under some adverse physiological conditions such as nutrient starvation, rapamycin treatment or osmotic, redox or thermal stresses, the activity of TORC1 is reduced considerably (Tate and Cooper 2013, Urban et al. 2007). Loss of TORC1 signaling triggers a starvation response in which protein synthesis decreases and autophagy is induced.

The upstream mechanisms by which adverse external conditions reach TORC1 and shut it down have been extensively studied (Loewith and Hall 2011), although it is still partially unclear. However, two main direct substrates of TORC1 have been described: the Sch9 protein kinase and the Tap42-phosphatases complex (Urban et al. 2007, Di Como and Arndt 1996), each belonging to separate downstream effector branches (Figure 1.7).

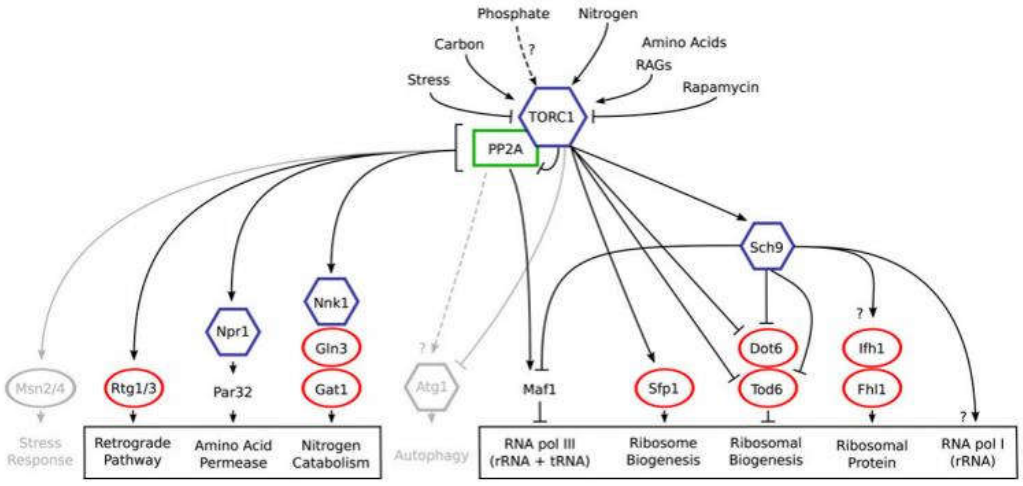

Figure 1.7. Schematic of the TORC1 downstream effectors and functions. TORC1 regulates numerous cell growth functions through a network of downstream effectors that influence protein and ribosome synthesis and a range of metabolic pathways. Kinases are shown in blue, phosphatases in green and transcription factors in red. (Hughes Hallett, Luo and Capaldi 2014).

The number of distal readouts downstream of TORC1 is higher (Breitkreutz et al. 2010). Among them the Npr1 kinase is central in the present work in its role as a negative regulator of endocytosis, as it stabilizes several PM permeases by antagonizing their Rsp5-mediated degradation (MacGurn et al. 2011).

6. Npr1 kinase

The nitrogen permease reactivator 1 (Npr1) was first identified based on its implication in the regulation of nitrogen permeases (Grenson and Dubois 1982). Currently, the role of Npr1 has been annotated as a regulator of many TORCs downstream biological processes, such as nitrogen utilization (De Craene, Soetens and Andre 2001), endocytosis and protein phosphorylation (MacGurn et al. 2011), sphingolipid biosynthetic processes (Shimobayashi et al. 2013) and transmembrane transporters activity (Vandenbol, Jauniaux and Grenson 1990).

Thus, Npr1 is a nutrient-regulated protein kinase that promotes the activity of diverse transport systems for nitrogenous nutrients under conditions of TORC1 activity inhibition.

6.1. Npr1 structure

Npr1 belongs to the Npr1/Hal5 subfamily of protein kinases (Hunter and Plowman 1997). Its complete structure has not been elucidated yet but it is known that its N-terminus includes a serine-rich domain with 26% serine content, while its C-terminus contains a serine/threonine kinase domain (Figure 1.8) (Vandenbol et al. 1990, Gander et al. 2009, MacGurn et al. 2011). Npr1 is constitutively expressed and its transcription is independent of the quality of the nitrogen source (Vandenbol et al. 1987).

6.2. Npr1 phosphorylation state and activity

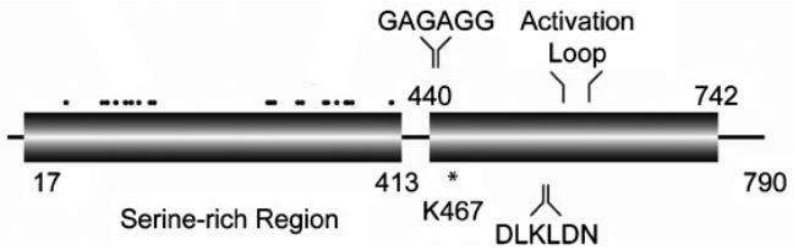

Figure 1.8. Npr1 putative structure. The N-terminal domain contains the serine-rich region (the filled circles represent the sites of phosphorylation) while the C-terminal contains de catalytic domain. (Gander et al., 2008).

A mass spectrometry analysis of Npr1 revealed 24 rapamycin-responsive phosphorylation sites within the N-terminal serine-rich domain (Bonenfant et al. 2003). Npr1 activity is regulated through its phosphorylation state, being active when dephosphorylated and inactive when phosphorylated (Schmidt et al. 1998). Normal TORC1 activity leads to phosphorylation of Npr1 while the absence of TORC1 signaling, such as in a medium with a poor nitrogen source or upon rapamycin treatment, leads to dephosphorylation of Npr1 (Jacinto et al. 2001). This regulation is known to involve a TORC1-dependent mechanism that involves both direct phosphorylation by TORC1 (Breitkreutz et al. 2010) and indirect control by regulation of phosphatases that dephosphorylate and activate Npr1 (Bonenfant et al. 2003).

6.2.1. Upstream phosphorylation of Npr1: Tco89

TORC1 is the only kinase complex known to phosphorylate Npr1. Multiple TORC1 subunits exhibit interactions with Npr1 (Breitkreutz et al. 2010). The Tco89 subunit is very rich in serine and threonine residues and is heavily phosphorylated in vivo (De Virgilio and Loewith 2006). The deletion of Tco89 is not lethal and cells lacking Tco89 show hypersensitivity to rapamycin (MacGurn et al. 2011). Npr1 phosphorylation has been shown to be deficient in strains lacking *TCO89* and therefore it has been

postulated that this subunit is involved in Npr1 substrate recognition by TORC1 (Crapeau, Merhi and André 2014).

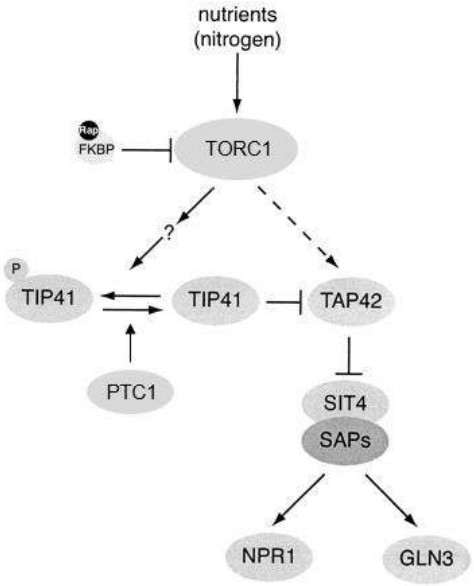

Figure 1.9. TORC1 controls phosphatases in *S. cerevisiae*. Under good nutrient conditions, TOR keeps the Sit4 phosphatase inactive by promoting its association to Tap42. Rap, rapamycin. Upon starvation or rapamycin, Sit4 is activated by dissociation from its regulatory subunit Tap42. The complex Tap42/Tip41 is thought to trigger the dephosphorylation of Npr1 by Sit4. The Ptc1 phosphatase ensures the normal levels of dephosphorylated Tip42, a protein proposed to be directly phosphorylated by TORC1. Image modified from Crespo and Hall, 2002.

6.2.2. Upstream dephosphorylation of Npr1: Sit4 and Ptc1

TORC1 indirectly controls the dephosphorylation of Npr1 by the means of the Tap42-phosphatase complexes. The type 2A-related phosphatase Sit4 is known to dephosphorylate Npr1 (Schmidt et al. 1998).This complex is regulated by TORC1 activity and has multiple associated functions. Tap42 is a well-conserved protein which interacts with the catalytic subunits of the type 2A and 2A-related phosphatases. (Di Como and Arndt 1996). Under conditions of normal TORC1 activity, Tap42 is phosphorylated and this promotes a functional association with 2A and 2A-like phoshpatases. When TORC1 is inactive, Tap42 is dephosphorylated and dissociates from the complex, releasing Sit4. Consequently, Sit4 is able to dephosphorylate Npr1 (Figure 1.9).

Type 2C Ser/Thr protein phosphatases (PP2C) are thought to ensure normal levels of the Tap42-interacting protein Tip41, whose complex is proposed to act as a specificity factor that would trigger the PP2A/Sit4-mediated dephosphorylation of Npr1 (Kuepfer et al. 2007). It has been observed that the absence of Ptc1 results in hyperphosphorylation of Npr1 (González et al. 2009).

6.3. Role of Npr1 in membrane remodeling

A consensus role for Npr1 in the trafficking of amino acid transporters has not yet been established. The effect of Npr1 activity is not equal on all of its target permeases, as it stimulates internalization of some and stabilizes others in the PM. For example, while one study presents evidence of the role of Npr1 promoting endocytosis of the tryptophan transporter Tat2 (Schmidt et al. 1998), other studies have found that it stabilizes transporters at the plasma membrane (De Craene et al. 2001). These contradictory reports evidence the lack of a global strategy by which TORC1 integrates the environmental cues with the Npr1-dependent membrane trafficking events. The scales may be tipping towards the role of Npr1 as a permease stabilizer, based on reports of the endocytosis regulation of Can1 by the TORC1 signaling pathway (MacGurn et al. 2011). A schematic representation of this model of Rsp5-mediated endocytosis regulation is described in Figure 1.10.

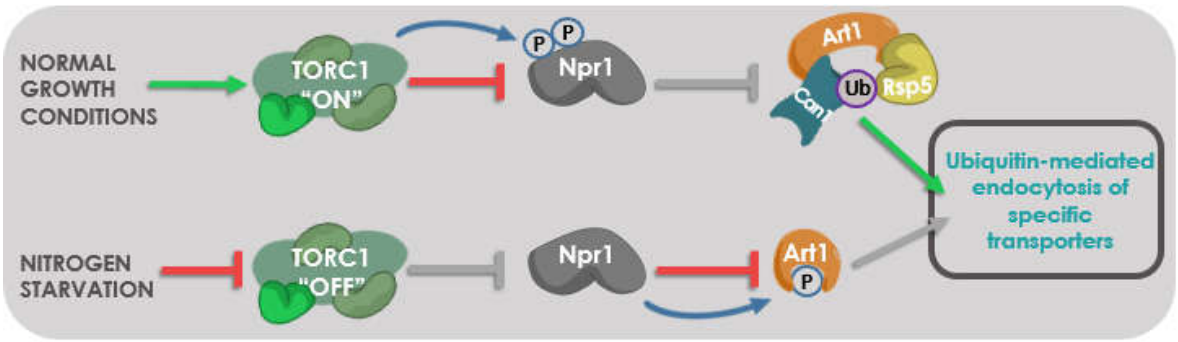

Figure 1.10. A mechanism for TORC1 regulation of endocytosis. When TORC signaling is "on" (top), Npr1 is phosphoinhibited which promotes endocytosis of specific transporters by promoting Art1-Rsp5 translocation to the PM. When TORC1 signaling is "off" (bottom), as occurs during rapamycin treatment or starvation conditions, Npr1 is active and can phosphorylate Art1, an inhibited state that prevents endocytosis. Gray arrows and bars indicate the release of a regulatory interaction due to upstream regulatory effects in the pathway. Simplified figure based on MacGurn et al., 2011.

Thus, there is clear evidence that Npr1 is a key regulator of the endocytosis of amino acid permeases through its regulation of members of the ART family of Rsp5 adaptors. In the case of Art1, Npr1 has been shown to act as a negative regulator, phosphoinhibiting Art1. However, the case of Art3 is less clear. We and others have observed a stable physical interaction between Nrp1 and Art3, but not Art1. Our preliminary data suggests that the Npr1-Art3 interaction may be rapamycin sensitive. Since the addition of this TORC1 inhibitor is known to lead to the dephosphorylation of Npr1 and also the phosphoinhibition of Art1, we postulate that the Npr1-Art3 interaction is dependent on the Npr1 phosphorylation state and that upon release of Npr1 from the Art3-containing complex, this kinase would be available to translocate to the plasma membrane where it could phosphoinhibit Art1 and lead to the stabilization of amino acid permeases, such as Can1. In the current project, we take several experimental approaches to begin to investigate this hypothesis.

Objectives

The objectives proposed for this project are as follows:

1. To further confirm the Npr1/Art3 interaction and its dependence on TORC1 signaling by studying its sensitivity to rapamycin.

2. To explore the hypothesis that the phosphorylation state of Npr1 determines its functionality on permease trafficking through different approaches:

    I. Measure the levels of plasma membrane permeases in a set of mutant strains with a described permanent effect on the phosphorylation state of Npr1:

        - Indirectly: observing its response to toxic amino acid analogues.

        - Directly: quantifying of the levels of the arginine permease Can1 by confocal microscopy and immunodetection.

    II. Study the subcellular localization of Npr1 in a set of mutant strains with a described permanent effect on its phosphorylation state.

Materials & Methods

Strains and Plasmids

Bacteria

All plasmids were amplified and extracted from pure bacterial cultures, using the DH5α strain of Escherichia coli. Bacterial cells were cultivated overnight at 37°C in Luria Bertani (LB) complex medium (10 g/L triptone, 5 g/L yeast extract and 0.17M sodium chloride, adjusted to pH 7.0 with NaOH). For solid medium, 2% agar was added. For plasmid selection 50 μg/mL ampicillin was added to both liquid and solid medium, as all of the plasmids used in this work contained the Amp resistance selection marker.

Yeast

The *Saccharomyces cerevisiae* strains used are listed in Table 3.1. Yeast cells were cultivated at 28°C in YPD complex medium (10 g/L yeast extract, 20 g/L peptone and 0.11M dextrose (glucose)) or SD minimum synthetic medium (2% glucose, 0.7% yeast nitrogen base without amino acids and 50mM succinic acid adjusted to pH 5.5 with Tris). In the case of the latter, different amino acids and purine and pyrimidine bases were added according to the strains' nutritional auxotrophies (30 μg/mL adenine, 30 μg/mL uracil, 30 μg/mL histidine, 10 μg/mL leucine, 10 μg/mL methionine and 10 μg/mL tryptophan).

Table 3.1. *S. cerevisiae* strains used in this work.

Strain	Information	Reference
THY.AP4	MATa; *ura3*, *leu2*, lexA::lacZ::*trp1* lexA::*HIS3* lexA::*ADE2*	Obrdlik et al., 2004
BY4741	MATa; *ura3*; *leu2*; *his3*; *met15*	EUROSCARF
npr1	BY4741 *npr1*::KanMX	EUROSCARF
tco89	BY4741 *tco89*::KanMX	EUROSCARF
sit4	BY4741 *sit4*::KanMX	EUROSCARF
ptc1	BY4741 *ptc1*::NatMX	Ruiz et al., 2006

The gene disrupted strains were tested according to their resistance to geneticin (G418, kanMX selection marker) or nourseothricin (natMX selection marker). The concentrations are shown in Table 3.3.

Table 3.2. Plasmids used in this work.

Plasmid	Information	Reference
pVT-100-*CAN1*-GFP	*CAN1*-GFP in 2µ URA3 marker, *ADH1* promoter	W. Tanner
pUG34-GFP	GFP in pUG34 *HIS3* marker, *MET25* promoter	V. Llopis
pUG34-GFP-*NPR1*	N-terminal *NPR1* fusion in pUG34-GFP	O. Sirozh
pRS411	CEN/ARS *MET15*	Brachmann et al., 1998
pACT2	2µ *LEU2* marker, *ADH1* promoter, N-terminal *GAL4* activation domain fusion, C-terminal HA tag fusion	P. Sanz
pACT2-*ART1*	*ART1* fusion in pACT2	J. Delás
pACT2-*ART3*	*ART3* fusion in pACT2	J. Delás
pBTM116	2µ *TRP1* marker, *ADH1* promoter, N-terminal LexA DNA binding domain fusion	P. Sanz
pBTM116-*NPR1*	NPR1 fusion in pBTM116	C. Primo
pBTM116-*RSP5*	WW domains *RSP5* fusion in pBTM116	L. Pedelini

Growth tests on solid media: Drop tests

A saturated overnight liquid culture of each strain was diluted to 1:10, 1:100 and 1:1000 in a multi-well plate. Approximately 3 µL of each dilution was transferred with a replicator (Sigma) to solid medium plates. The plates were then grown at 28°C over 3 days or longer, as the growth rate was different for each strain and condition. All the conditions tested in this work are compiled in Table 3.3.

Table 3.3. Summary table of the solid medium treatments used in this work.

Product	Description	Medium	Treatment
Azetidine-2-carboxylic acid (AzC)	Toxic proline analogue	SD	0.5 and 1 mM
L-Canavanine	Toxic arginine analogue	SD	1, 2 and 3 µg/mL
Geneticin (GEN)	Aminoglycoside antibiotic	YPD	200 µg/mL
Nourseothricin (NTC)	Aminoglycoside antibiotic	YPD	100 µg/mL
Rapamycin (RAP)	Macrolide antibiotic TOR pathway inhibitor	YPD	1, 2.5, 5, 10 and 20 ng/mL

Yeast transformation

For each transformation, 5 µL of ssDNA (1%, preheated at 95°C for 5 min) and 1.5 – 4 µg of each plasmid (generally 5 – 10 µL of plasmids at 200 – 600 ng/mL) were mixed with sterile Mili-Q water to a final volume of 50 µL. Biomass of the appropriate strain (freshly grown on an YPD plate for no longer than 48h) was collected with a 1 µL inoculation loop and introduced in the previous solution. This was followed by the addition of 500 µL of PLATE solution (40% PEG-4000, 100 mM lithium acetate (LiAc), 10 mM Tris pH 7.5, 0.4 mM EDTA).

After incubating overnight at room temperature, the samples were incubated at 42°C for 15 min and the cells were collected by centrifugation (2 min, 15,700 *g*). Finally, they were resuspended in 200 µL of sterile Mili-Q water and plated onto appropriate selection medium according to their nutritional auxotrophies and the plasmids used.

Plasmid extraction from *E. coli* (Mini-prep)

The extraction and purification of plasmids was carried out using the NucleoSpin® Plasmid EasyPure kit (Macherey-Nagel). This method combines an initial phase of a SDS/alkaline bacterial lysis with a column purification of the plasmid DNA.

Parting from 5 mL of a saturated pre-culture of transformed *E. coli* grown overnight at 37°C in selection medium, the cells were collected by centrifugation at maximum speed. The pelleted cells were resuspended in 150 µL of *Resuspension Buffer A1* containing RNase A and were lysed by the addition of 250 µL of *Lysis Buffer A2*, inversion of the tubes and 2 min incubation at room temperature. This phase was finalized by the addition of 350 µL of *Neutralization Buffer A3*. Precipitated protein, genomic DNA, and cell debris were then pelleted by centrifugation (3 min, 15,700 *g*). The supernatant was then loaded onto a NucleoSpin® Plasmid EasyPure Column and centrifuged for 30 seconds at 1,000 – 2,000 *g*, after which the flow-through was discarded. The column was washed by the addition of 450 µL of *AQ Washing Buffer* and a centrifugation step (1 min, 1,800 *g*). Finally, the plasmid DNA was eluted from the column with 50 µL of *AE Elution Buffer* and a last centrifugation step (1 min, 15,700 *g*).

The efficiency of the extractions was assessed by digesting the plasmids with appropriate restriction enzymes and visualizing the result using electrophoresis on a 0.8% ethidium bromide-stained agarose gel.

Protein Analysis

Total protein extract

Yeast cultures were inoculated in appropriate selection media using saturated pre-cultures grown overnight at 28°C. The biomass was recovered at logarithmic phase (OD595 = 0.5 - 0.6) by centrifugation (1500 *g* for 5 minutes), and washed with sterile water. The biomass was resuspended in 50 µL of Laemmli loading buffer 2.5X (3.8% SDS, 0.05 M dithioeritritol, 5 mM EDTA, 15% sucrose, 0.125 mg/mL bromophenol blue, 0.15 M Tris-HCl pH 6.8) and incubated for 5 minutes at 95°C.

TCA Method

Yeast cultures were inoculated in appropriate selection media using saturated pre-cultures grown overnight at 28°C. Cells were grown to logarithmic phase (OD595 = 0.5 - 0.6) and 0.6 mL of 100% (w/v) Trichloroacetic acid (TCA) were added to 10 mL of culture. This mixture was put on ice for at least 5 min. Then the biomass was recollected by centrifugation (5 min, 1,500 *g*) and transferred to screw cap micro tubes. After another pelleting step (2 min, 15,700 *g*, 4°C), the cells were washed twice with 0.5 mL of cold acetone (2 min, 15,700 *g*, 4°C). The samples were dried out in a Speed vac. centrifuge (10 min). Once dry, 100 µl of Urea buffer (25 mM Tris-HCl pH 6.8, 6 M Urea, 1% SDS) were added together with 200 µl of glass beads (0.5 mm diameter) and the cells were lysed by agitation in a Mini Bead beater (BioSpec Products) in 5 cycles of 45 s. The samples were heated up to 65°C in a thermoblock for 5 min and centrifuged (5 min, 15,700 *g*). After the addition of 100 µl of Laemmli loading buffer 2X (3.8% SDS, 0.05 M dithioeritritol, 5 mM EDTA, 15% sucrose, 0.125 mg/mL bromophenol blue, 0.15 M Tris-HCl pH 6.8) the samples were briefly vortexed and again centrifuged (5 min, 15,700 *g*). An appropriate amount of supernatant was loaded on an SDS-PAGE gel, after it was heated to 95°C in a thermoblock for 5 min.

Protein electrophoresis

The protein separation through electrophoresis was carried out in polyacrylamide gels under denaturing conditions (SDS-PAGE) using the Mini-PROTEAN® 3 System (BioRad). The proteins were separated using a biphasic polyacrylamide gel containing a superior stacking phase (6-8% acrylamide:bisacrylamide, 125 mM Tris-HCl pH 6.8 and 0.1% SDS) and a lower resolving phase (10% acrylamide:bisacrylamide, 375 mM Tris-HCl pH 8.8 and 0.1% SDS). The electrophoresis was carried out in SDS-PAGE Buffer 1X (0.19 M glycine, 0.1% SDS, pH 8.3 adjusted with Tris). The samples were first ran under a potential difference of 80 V until they entered the resolving gel, then the voltage was increased to 120 V.

In order to identify the size of the proteins separated in the electrophoresis gel, 5 µL of the PageRuler™ Prestained Protein Ladder (Thermo Scientific) were added to a well, according to the manufacturer's indications for the well thickness (1.5 mm).

Electrotransfer to nitrocellulose membrane (Western blot)

Once the proteins were separated, they were transferred to the surface of a nitrocellulose membrane (Millipore) using the Mini Trans-Blot® Electrophoretic Transfer System (BioRad). The transfer was carried out in TOWBIN Buffer (0.19 M glycine, 0.01% SDS, 20% methanol, pH 8.3 adjusted with Tris) under a constant potential difference of 120 V for 1.5-2h or until the current exceeded 300 mA, at 4°C.

Direct Blue staining

In order to verify the efficiency of the transfer and as an internal loading control, the membranes were stained with Direct Blue (Aldrich Chemistry) after the transfer. The nitrocellulose membranes were submerged in a Staining Solution (0.008% [w/v] DB71, 40% ethanol and 10% acetic acid) for 5 min on a rocker. To eliminate the excess dye the membranes were submerged in a Washing Solution (40% absolute ethanol and 10% glacial acetic acid). After obtaining a digital image (the

membranes were wrapped in plastic and scanned), the Direct Blue dye was eliminated with a Destaining Solution (50% absolute ethanol and 150mM sodium bicarbonate (NaHCO3)).

Inmunodetection of the transferred proteins

In order to avoid non-specific antibody binding, the membranes were submerged in a Blocking Solution (2% non-fat milk in TBS-Tween Solution (150 mM NaCl, 20 mM Tris-HCl pH 7.6 and 0.1% Tween 20)) during at least 30 min. The primary antibody was administered in the blocking solution at the necessary concentration (Table 3.4), and incubated on a rocker overnight, at 4°C. The membrane was then washed three times for 10 minutes each with TBS-Tween Solution and incubated with the secondary antibody for 1h, at RT. Finally, the washing steps were repeated.

Table 3.4. Antibodies used in this work.

Primary antibody	Dilution	Source	Secondary antibody	Dilution	Source
α-lexA	1:20000	Abcam	*a*-HRP-rabbit	1:10000	Amersham
α-GST	1:2500	Santa Cruz Biotechnology	*a*-HRP-rabbit	1:10000	Amersham
α-GFP	1:5000	Roche	*a*-HRP-mouse	1:10000	Amersham

The secondary antibody was detected by chemoluminiscence using the ECL Plus Western Blotting Detection System (Amerhsam Biosciences). The detection reagents A and B were mixed 1:1, as indicated by the manufacturer. The mixture was applied on the membrane and incubated for 5 min. After draining the excess, the membrane was introduced in a fresh plastic wrap and placed in an X-ray film cassette for exposure to a radiography film (Biomax Light-1, Kodak). The time of exposure was adjusted to the intensity of the signal.

When the detection with more than one antibody was needed, the membrane (stored at -20°C) was submerged in a Stripping solution (100 mM β-mercaptoethanol, 2% SDS and 6.25 mM Tris-HCl pH 6.7) followed by washing three times for 10 minutes each with the TBS-Tween solution.

Confocal microscopy

Fluorescence images were obtained for live cells grown to exponential phase in minimal media using either the Zeiss 780 confocal microscope with excitation at 488 nm and detection at 510-550 nm for GFP (objective: plan-apochromat 40X/1.3 OIL DIC M27, Zeiss ZEN 2012 software).

Results

1. Study of the interaction between Npr1 and Art3: effects of TORC1 signaling

A possible physical interaction between Npr1 and Art3 was first described to happen based on the analysis of Art3 co-purifying proteins by mass spectrometry. This interaction was verified by reciprocal co-purifications of Npr1-Myc through immunoprecipitation and Art3-GST through affinity chromatography (O'Donnell et al. 2010). In addition, it was also found that Npr1 can phosphorylate Art3 in vitro, based on differential electrophoretic mobility in SDS-PAGE gels. It was later confirmed that Art3 is phosphorylated in an Npr1-dependent manner by quantitative mass spectrometry (MacGurn et al. 2011).

The function of Npr1 as a TORC1 effector is controlled negatively through phosphorylation. Under normal growth conditions, Npr1 is constitutively phosphorylated in a TORC1-dependent manner and is inactive, whereas upon nitrogen limitation or rapamycin treatment TORC1 is inhibited and thus Npr1 is weakly phosphorylated and active (Schmidt et al. 1998).

The effect of rapamycin on the Npr1/Art3 interaction: Yeast-Two-Hybrid assay

A yeast-two-hybrid (Y2H) assay was used to confirm the interaction and observe the implication of TORC1 signaling. This was tested by examining the effect of rapamycin, a compound known to stimulate Npr1 kinase activity via inhibition of TORC1 (Gander et al. 2008).

The vectors containing the activation domain (pACTII) and the DNA binding domain (pBTM116) (Table 3.2 of Materials & Methods) were co-transformed into the *S. cerevisiae* THY.AP4 genetic background strain (Obrdlik et al. 2004), generating the set of transformed strains used in this Y2H assay. These strains were grown on SD plates with increasing concentration of rapamycin (Table 3.3 of Materials & Methods).

As observed in Figure 4.1, the different transformants in SD –L –W without rapamycin had similar cell growth, while on SD –L –W –H –A only the THY.AP4 [*NPR1*][*ART3*] strain showed observable levels of growth, indicating a strong physical interaction between Npr1 and Art3, which decreased in the presence of increasing concentrations of rapamycin. The 2.5 ng/mL treatment did not present changes, however under the 5 and 7.5 ng/mL treatments the growth was reduced on the SD –L –W –H –A plates in comparison with the SD –L –W. This reduction even reached the point where the interacting strains presented less growth than the control strain containing the empty vectors in the presence of 7.5 ng/mL rapamycin. This result may suggest that upon rapamycin treatment, which decreases Npr1 phosphorylation, the interaction between Art3 and Npr1 decreases. Npr1 might be liberated in order to phosphorylate Art1.

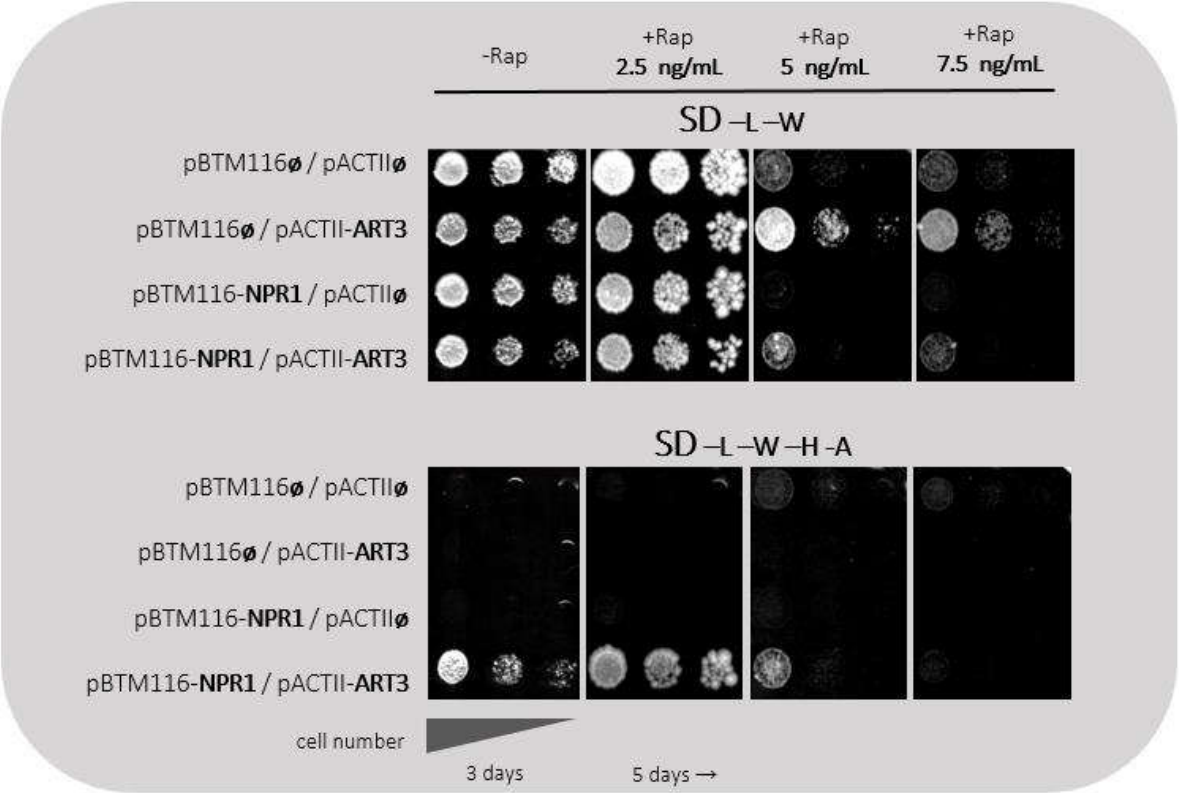

Figure 4.1. Yeast-Two-Hybrid assay of Npr1- Art3 interaction and controls. The THY.AP4 genetic background was transformed with the plasmids indicated in the figure. The resulting transformants were grown to saturation in SD –L –W and, after serial dilutions, drops were placed on solid plates containing the indicated supplements: SD media –L –W and SD media –L –W –H –A with increasing concentrations of rapamycin (2.5 ng/mL, 5 ng/mL and 7.5 ng/mL). Three independent clones were analyzed with same results. Abbreviations: Rap, rapamycin.

In this experiment, we also confirmed the tolerance to rapamycin mediated by *ART3* overexpression (O'Donnell et al. 2010). Another interesting observation stemming from this Y2H assay was the ability of Art3 to act as a suppressor of *NPR1*-mediated toxicity in the presence of rapamycin. The strain expressing Npr1 alone grew very poorly in the presence of rapamycin, whereas some growth was recovered in the strains co-expressing Npr1 and Art3. This result may suggest that Art3 attenuates an Npr1 activity that is detrimental in the presence of rapamycin.

In order to further verify if the reduction in the growth of the Npr1-Art3 strains upon rapamycin treatment was due to the destabilization of its physical interaction, a set of control strains were also generated. On one hand, we used another ART protein, Art1, which is known to be a direct Npr1 substrate as well. However these proteins do not physically interact (MacGurn et al. 2011). The combination of these proteins was used as a negative control in the Y2H. On the other hand the E3 ubiquitin ligase Rsp5 is known to bind the ART proteins and use them as adaptors for ubiquitylation of its substrates. The Rsp5 WW domains physically interact *in vivo* with the PY motifs of Art3 (Hatakeyama et al. 2010), as well as with Art1 (Lin et al. 2008). Therefore, the combination of these proteins was used as a positive control for the Y2H.

As observed in Figure 4.2, again the strains growing in SD –L –W without rapamycin showed similar levels of growth. However, we observed a similar growth profile in SD –L –W –H –A for the *RSP5* strains co-transformed with *ART1*, *ART3* and also the empty vector. This result is likely to be explained by transactivation of the *RSP5* construct. Therefore, although it is well known that ART

proteins interact with the WW domain of Rsp5, the Y2H approach does not appear to be adequate to study these interactions. Nevertheless, the fact that all three strains presented similar levels of growth in the presence of 5 ng/mL rapamycin is consistent with, but not conclusive of a specific effect of this treatment on the Npr1-Art3 interaction observed above.

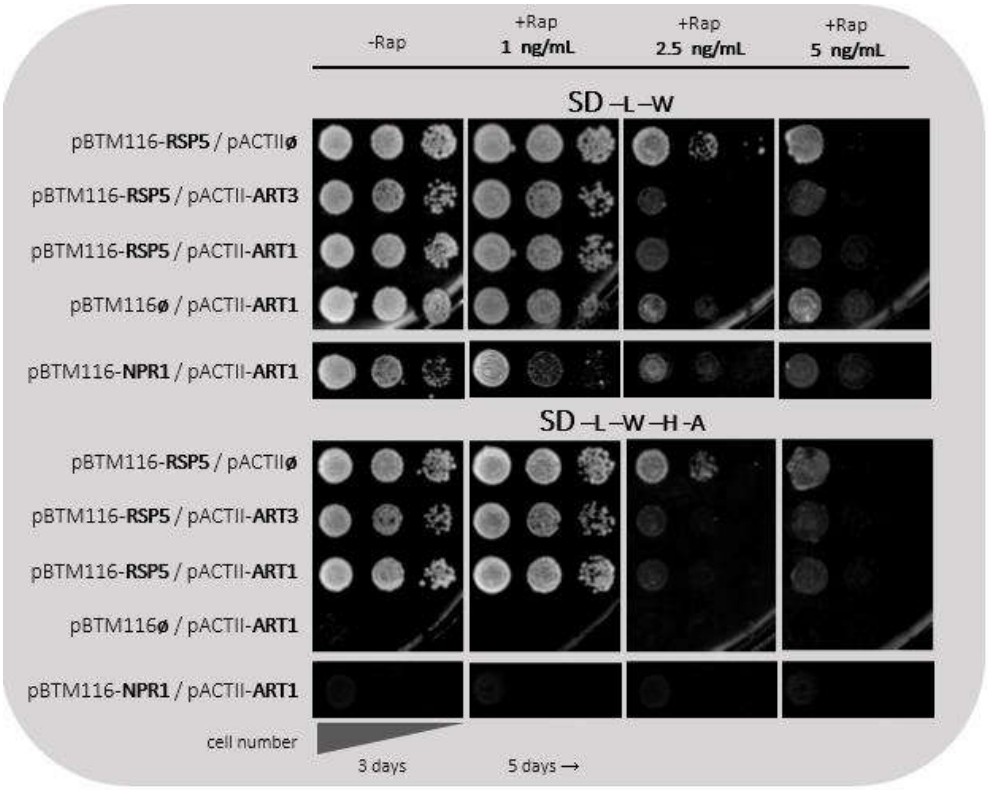

Figure 4.2. Yeast-Two-Hybrid assay of a set of positive and negative interaction controls. The THY.AP4 genetic background was transformed with the plasmids indicated in the figure. The resulting transformants were grown to saturation in SD –L –W and, after serial dilutions, drops were placed on solid plates with the indicated supplements: SD media –L –W and SD media –L –W –H –A with increasing concentrations of rapamycin (1 ng/mL, 2.5 ng/mL and 5 ng/mL). Three independent clones were analyzed with same results. Abbreviations: Rap, rapamycin.

In addition, it was also confirmed that Npr1 does not need to interact with Art1 in order to phosphorylate this substrate, as was observed an important lag in growth of the THY.AP4 [NPR1][ART1] strain on SD –L –W –H –A compared to growth on SD –L –W. The expression of the proteins of each strain was confirmed by western blot as described in Materials & Methods for the Npr1, Art3, Art1 (Figure 4.3) and Rsp5 transformants (data not shown).

These observations support previous results obtained in our laboratory showing a rapamycin sensitive interaction of the robust association between the N terminal fragment of Art3 and Npr1 (Sirozh, 2015). The tentative hypothesis that can be drawn from the experiments described above contends that Npr1 binding and subsequent phosphorylation of ART proteins may depend on its phosphorylation level. Npr1 may interact physically with Art3 under conditions where Npr1 is phosphorylated, whereas it may be released and capable of phosphorylating Art1 upon dephosphorylation, induced here by rapamycin treatment.

In the following sections we explored this hypothesis to determine whether a correlation exists between the phosphorylation state of Npr1 and its functionality.

2. Study of the effects of the phosphorylation state of Npr1 on membrane trafficking

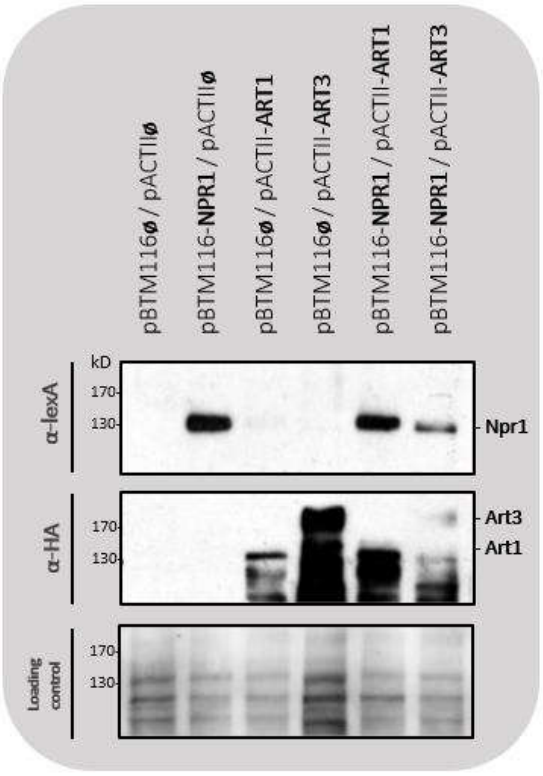

Figure 4.3. Western blot analysis of the Y2H strains. The THY.AP4 genetic background was transformed with the plasmids indicated in the figure and grown to exponential phase in SD medium. The total protein content was extracted and samples were run on an 8% SDS-PAGE gel. The transfer, immunodetection and stripping were performed as described in Materials & Methods. The molecular weight markers appear on the left side of the figure (kDa). The Direct Blue staining of the membrane is shown as a loading control.

A model presenting a mechanism by which TORC1 regulates endocytosis via Npr1-mediated phosphoinhibition of Art1 (MacGurn et al., 2011) has been used in this project as a platform to study whether a correlation between the function of Npr1 as a permease trafficking regulator and its phosphorylation state. The basis for this approach was the use of a set of mutant strains with a described permanent effect on the phosphorylation state of Npr1. Different kinases and phosphatases were selected based on previous evidence regarding Npr1 phosphorylation (described more extensively in the Introduction, section 6.2). Genetically disrupted strains in the BY4741 genetic background for these genes were used as our analysis group as well as a strain lacking the *NPR1* gene (Table 3.1 of Materials & Methods). Specifically, we employed a set of strains composed by the mutant for the Npr1 kinase (*npr1*), the Tco89 TORC1 subunit (*tco89*) and the mutants for the Sit4 (*sit4*) and the Ptc1 phosphatases (*ptc1*), which have been described to dephosphorylate Npr1 directly and indirectly, respectively.

The exploration of the hypothesis presented above was carried out through a series of experiments run in parallel. The phenotype of the mutants was first characterized based on previous observations and thereafter three independent approaches were set up:

I. Response to toxic amino acid analogues as a measure of plasma membrane accumulation of amino acid permeases.
II. Direct analysis of the plasma membrane accumulation of the Art1-dependent Can1 arginine permease by confocal microscopy and immunodetection.
III. Analysis of the phosphorylation state and subcellular localization of Npr1.

We characterized and quantified the subcellular location of the arginine permease Can1 by confocal microscopy based on evidence that this transporter is localized in the PM when Npr1 is activated. The differential electrophoretic mobility of Npr1 and its influence to rapamycin was also analyzed in the different mutant strains. At the same time the subcellular location of Npr1 in these

strains was also studied, as was its response to rapamycin by confocal microscopy and the morphological characterization of these cells when transformed with GFP alone.

Genetic manipulation of the phosphorylation state of Npr1: Genotypic and phenotypic- characterization of the selected mutant strains

In order to investigate a correlation between the role of this kinase as a membrane traffic regulator and this post-translational modification, Npr1 hypophosphorylation and hyperphosphorylation states were artificially recreated by using a selected set of gene-disrupted strains.

Genotype analysis

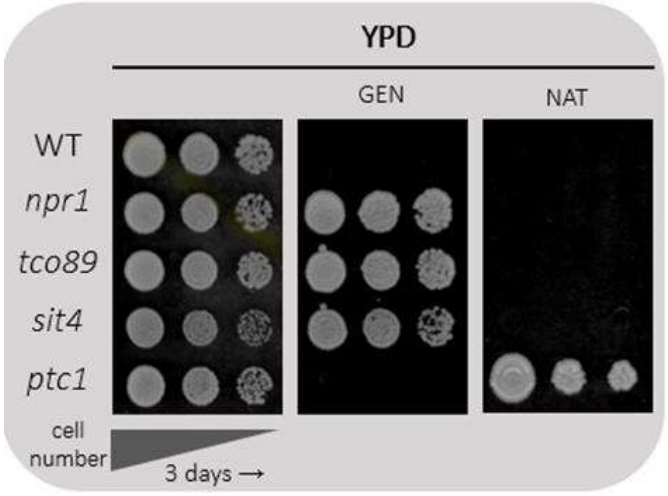

Figure 4.4. Growth genotypes of the indicated mutants of the BY4741 genetic background. Cells were grown to saturation on YPD and, after serial dilutions, drops were placed on solid media with geneticin and nourseothricin. Two independent clones were analyzed with same results. Abbreviations: Rap, rapamycin.

An initial genotypic and phenotypic characterization of our set of strains was carried out through drop tests under different conditions (Table 3.3 of Materials & Methods). The mutant genotypes were confirmed through the antibiotic selection gene contained in their disruption cassettes according to their resistance to geneticin (kanMX selection marker) or nourseothricin (natMX selection marker) (Table 3.1 of Materials & Methods). As observed in Figure 4.4 the mutant strains presented the correct genotypes, observing no growth of the wild type in either antibiotic.

Rapamycin growth phenotype

The phenotypes of the mutant strains in the presence of rapamycin were also examined. In Figure 4.5, the tolerance of the *npr1* to all the concentrations of rapamycin in comparison to the wild type can be observed, indicating that the absence of this protein makes the cells highly resistant to this compound. Resistance to rapamycin was also observed for the *sit4* mutant strains. On the contrary, the absence of the Tco89 TORC1 subunit rendered the cells hypersensitive to rapamycin, as observed in the absence of growth of *tco89,* even in the presence of 2.5 ng/mL rapamycin. Sensitivity to this compound was also observed for the *ptc1* mutant.

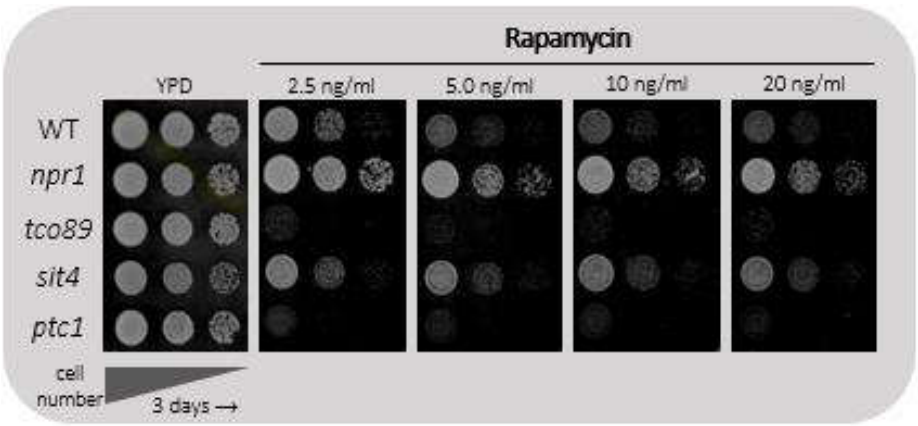

Figure 4.5. Rapamycin growth phenotypes of the wild-type and indicated mutants of the BY4741 genetic background. Cells were grown to saturation on YPD and, after serial dilutions, culture drops were placed over solid plates with increasing concentrations of rapamycin (2.5 ng/mL, 5 ng/mL, 10 ng/mL and 20 ng/mL). Two independent clones were analyzed with same results. Abbreviations: Rap, rapamycin.

These results suggest that lack of Npr1 activity, either by gene deletion or increased phosphorylation by removal of the *sit4* phosphatase leads to rapamycin resistance, whereas over-activation of Npr1, which would be predicted for the *tco89* mutant in which Npr1 phosphorylation has been shown to be reduced, is detrimental for growth in the presence of rapamycin. This interpretation is further supported by the results reported above for strains overexpressing *NPR1* (Figure 4.1). However, the phenotype of the *ptc1* mutant does not fit with the proposed hypothesis. Previous studies have suggested that Npr1 is highly phosphorylated in strains lacking Ptc1, similar to that observed for the *sit4* mutant, but the mutant strains lacking these phosphatases shown opposite phenotypes in terms of rapamycin response. This suggests that other Ptc1 activities are influencing its tolerance to rapamycin.

I. Growth response to toxic amino acid analogues

As discussed above, previous studies show that the arginine transporter Can1 is stabilized by Npr1 in the plasma membrane upon nitrogen starvation or rapamycin treatment (MacGurn et al., 2011). This stabilization is due to the phosphoinhibition of Art1 by the active Npr1 kinase, which prevents Rsp5-dependent ubiquitylation and subsequent vacuolar degradation of the permease. One convenient way to test for the accumulation of amino acid permeases at the plasma membrane is the use of toxic amino acid analogues, such as canavanine and azetidine carboxylic acid (AzC). These are toxic analogues of arginine and proline, respectively. AzC enters cells through several permeases, including Gap1 and Put4, whereas canavanine enters via the Can1 permease (Andréasson et al., 2004; Grenson et al., 1966). Cell sensitivity to these compounds is a convenient read-out of PM localization and activity of these permeases.

To observe the downstream effects of modifying the phosphorylation state of Npr1 in regulating endocytosis, trafficking and activity of amino acid permeases, the set of mutants was grown in the presence these toxic amino acid analogues (Table 3.3 of Materials & Methods).

Based on the model of Npr1 function, we would predict that lack of Npr1 activity (*npr1, sit4, ptc1*) would lead to Art1 mediated degradation of the amino acid permeases, which is predicted to confer tolerance to the toxic amino acid analogues. On the other hand, activation of Npr1 (*tco89*) should lead to Art1 phosphoinhibition, permease accumulation in the plasma membrane and the subsequent sensitivity to the toxic analogues. The growth profiles of the strains are presented in Figure 4.6. We observed the expected growth profile for the *npr1* and *tco89* strains, however, the strains lacking the phosphatase genes are surprisingly sensitive to both compounds. These results may indicate that additional effects of the lack of these phosphatase genes are influencing their response to these compounds.

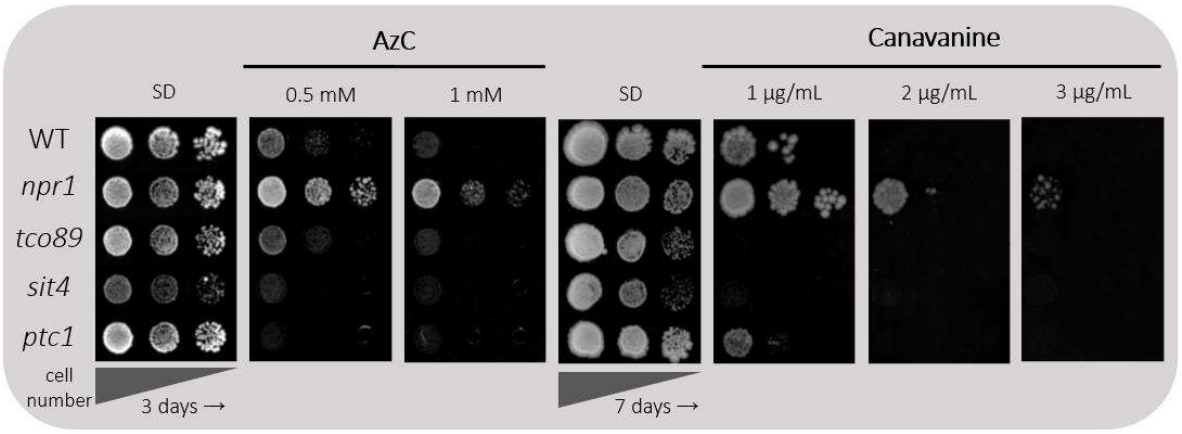

Figure 4.6. AzC and canavanine growth phenotypes of the wild-type and indicated mutants of the BY4741 genetic background. Cells were grown to saturation on SD and, after serial dilutions, culture drops were placed over solid plates with increasing concentrations of AzC (0.5 mM and 1 mM) and canavanine (1 µg/mL, 2 µg/mL, 3µg/mL). Two independent clones were analyzed with same results.

II. Study of the subcellular localization of Can1 in the mutant strains by fluorescence microscopy and immunodetection

The results presented above for the toxic amino acid analogues are not fully consistent with the model for Npr1 function. However, as mentioned, it is possible that the absence of the *SIT4* and *PTC1* phosphatase genes could lead to additional phenotypes affecting their response to these compounds. Therefore, to complete this analysis, in parallel, we examined the accumulation and subcellular localization of Can1 directly using two approaches: confocal microscopy and immunodetection.

As described in Materials and Methods, a wild-type BY4741 strain and the set of mutant strains were transformed with the pVT100-Can1-GFP plasmid (Table 3.2 of Materials & Methods). The cultures were grown to exponential phase and the expression and localization of the Can1-GFP fusion protein was observed by fluorescence microscopy.

As observed in Figure 4.7, all of the strains presented Can1-GFP in the plasma membrane. The PM distribution in the wild-type strains was not homogeneous as it presented accumulations in punctate regions. This localization has been described previously to correspond to microdomains of the plasma membrane which differ in their lipid and protein content (Grossmann et al. 2008). The localization in the *npr1* and *tco89* strains was both in the membrane and cell interior, where it was even possible to detect the shape of the nucleus (without fluorescence inside) and of fluorescent vacuolar compartments. The *sit4* strain was, in comparison, the one showing less cell interior fluorescence and a very well defined membrane with homogeneous Can1-GFP distribution that permitted the appreciation of a distinctive more elongated cellular shape. The *tco89* and *ptc1* mutant strains presented very low Can1-GFP expression and its fluorescence levels in the presented images were adjusted to the other strains for comparative reasons.

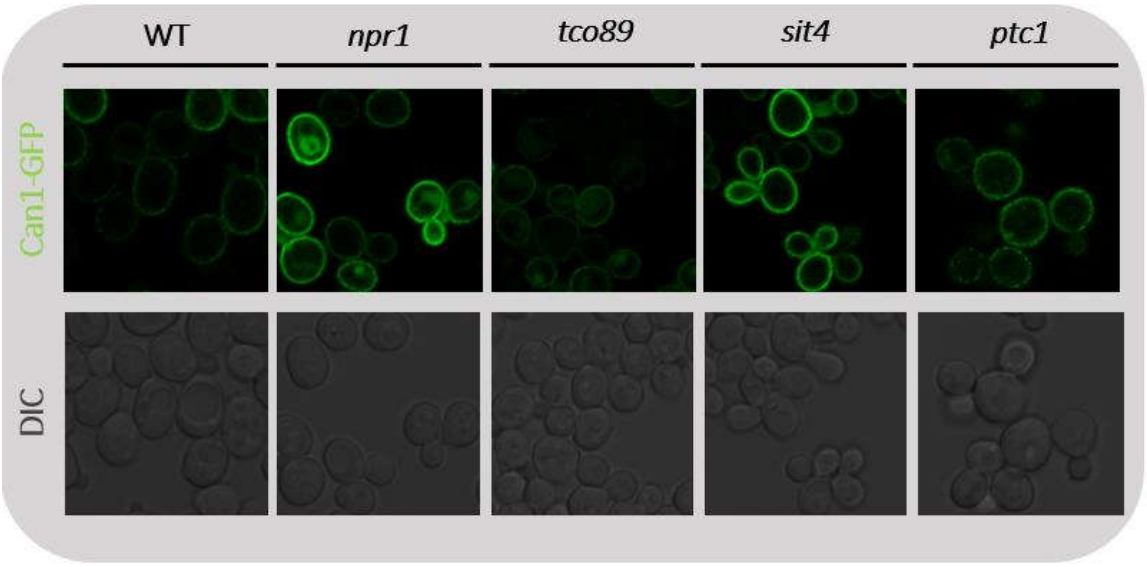

Figure 4.7. Subcellular localization of the arginine permease Can1-GFP in the wild-type and indicated mutants of the BY4741 genetic background. Confocal microscopy images of the subcellular localization of the fusion protein Can1-GFP in the indicated strains. The transformed cells were grown in SD medium to exponential phase and visualized by confocal microscopy. Representative images are shown. Similar phenotypes were observed in three different clones.

The PM-associated fluorescence was calculated for each strain as indicated in Figure 4.8B. Previous results showed differential Can1-GFP presence in the PM in the WT and *npr1* strains, with the internal fluorescence of *npr1* two-fold higher than the WT (MacGurn et al. 2011). Moreover, the model for Npr1 function would predict both the *sit4* and *ptc1* mutants to have lower amounts of Can1 in the PM, whereas the *tco89* mutant should show Can1 plasma membrane accumulation. On the other hand, based on the canavanine resistance profile, we would predict the *npr1* mutant to have decreased Can1 and the rest of the mutants to present increased amounts of the permease at the plasma membrane.

The fluorescence populations were analyzed and are presented in the Box and Whiskers plot in Figure 4.8A. We observed that the WT, *npr1* and *tco98* strains presented similar PM-localized Can1-GFP amounts. Significant differences were only found in the *sit4* strain. In this case, there was a higher Can1 proportion in the PM, which is consistent with the canavanine sensitivity of this mutant but not with the predicted inactivation of Npr1. The *ptc1* data was included, but it was only possible to quantify 10 cells and so no solid conclusions can be made in this case.

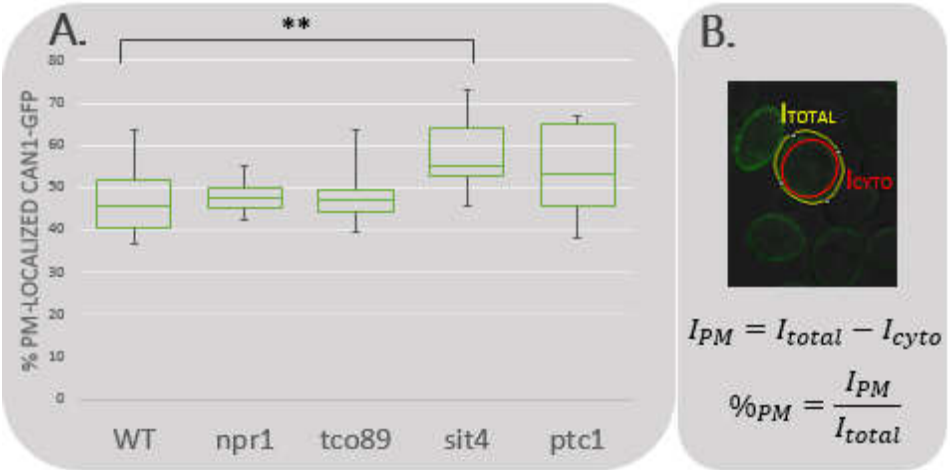

Figure 4.8. Quantification of the PM localization of Can1-GFP. (A) Box and Whiskers diagram of the percentages of PM-localized Can1-GFP in the different strains. The statistical significance of the data was studied by t-test. The asterisk (**) indicates significant differences with a p value < 0.001. (B) The quantification was performed as shown in the figure (n > 40), excluding *ptc1* (n=10).

According to these results, the genetically modified phosphorylation state of Npr1 did not show a correlation with the amount of the arginine permease Can1. Our data thus contrasts with the previous published results described above. However, it must be stated that this analysis only reports on the relative distribution of the Can1 permease. This analysis is not appropriate to determine total levels of the protein. In order to determine the total amount of protein, immunodetection assays were carried out and the results are presented in Figure 4.9A. In addition, all of the transformants were verified by their antibiotic resistances and by their growth phenotypes in rapamycin (Figure 4.9B).

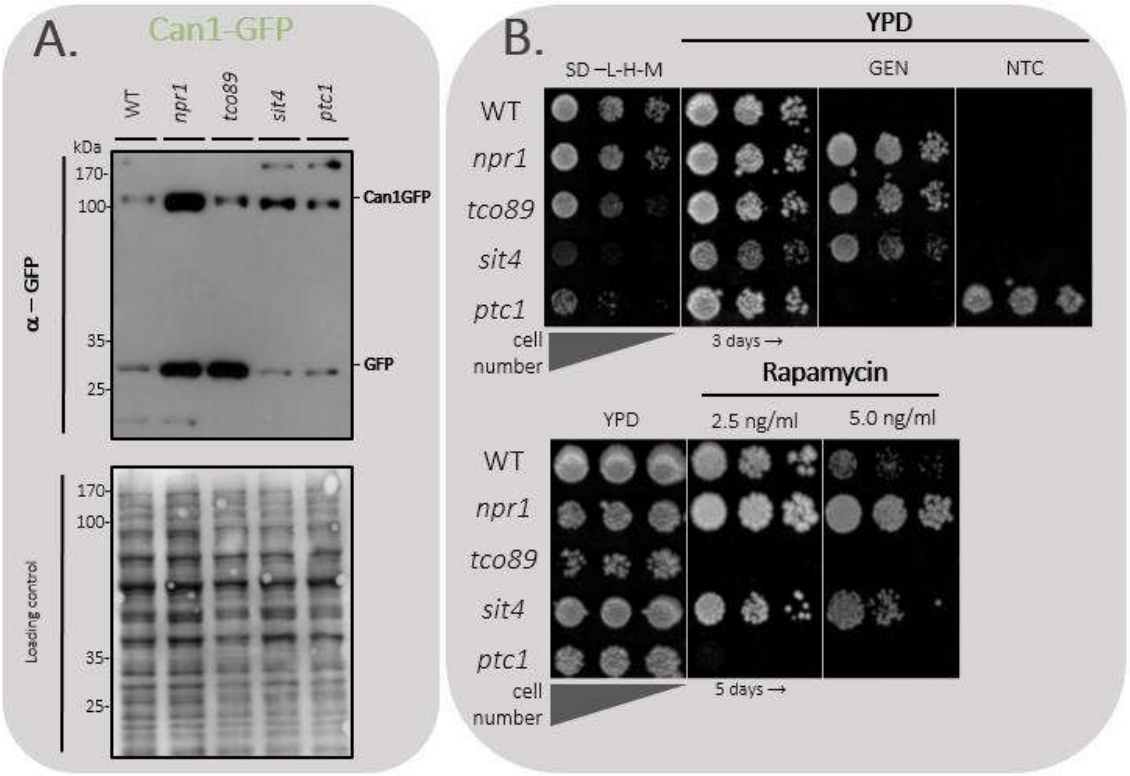

Figure 4.9. (A) Western blot analysis of Can1-GFP expression levels. The indicated strains were transformed with the pVT-100-Can1-GFP plasmid and grown to exponential phase in SD medium. The TCA method was used for the extraction of the total protein content. Samples were run on an 8% SDS-PAGE gel and the transfer and immunodetection were performed as described in Materials & Methods. The molecular weight markers appear on the left side of the figure (kDa).The Direct Blue staining of the membrane is shown as a loading control. **(B) Genotypic and phenotypic confirmation of Can1-GFP transformants.** The resulting transformants were grown to saturation in SD –L –H –M and, after serial dilutions, drops were placed on solid plates with the compounds indicated in the figure. Both genotypic and phenotypic growth tests in rapamycin were performed. Two clones were analyzed with same results. Abbreviations: GEN, geneticin; NTC; nourseothricin.

Contrary to what would be expected, higher Can1 levels were observed in the *npr1* mutant, as compared to the wild type control. The reason for this discrepancy is unknown, but it would be necessary to test more clones in order to make a firm conclusion. On the other hand, the *tco89* mutant showed a lower relative amount of full-length Can1 (ratio between the band at 110 kDa vs. the free GFP band at 27 kDa), but the total amount of full length Can1 was similar to that observed

in the wild type control. The same was true for both phosphatase mutants. Interestingly, both phosphatase mutants present an additional band at 180 kDa. However, this was not observed in all experiments. In conclusion, we fail to observe a correlation between either the predicted phosphorylation state of Npr1 and Can1 levels in the mutant strains, or between the canavanine resistance and Can1 accumulation. These results are very surprising and difficult to interpret, but clearly indicate that the final result of the chosen assays is more complex than what could be predicted from the proposed model of Npr1 function.

III. Study of the subcellular localization of Npr1 in the mutant strains by fluorescence microscopy

The third and final approach of this analysis was based on the described change in co-localization of Art1 and Npr1 upon a rapamycin treatment (MacGurn et al. 2011). While in unstimulated wild-type cells Art1 localizes in the cytosol, Golgi and PM, the addition of rapamycin partially inhibits the PM recruitment of Art1. These differences correlate with the phosphorylation state of Art1. The subcellular localization of Npr1 was also characterized under these conditions, changing from exclusively cytosolic towards the PM upon rapamycin treatment. Taking into account that Art1 is a target of Npr1 phosphorylation, it was also observed that a rapamycin treatment triggered the transitory co-localization of Npr1 and Art1 in the PM.

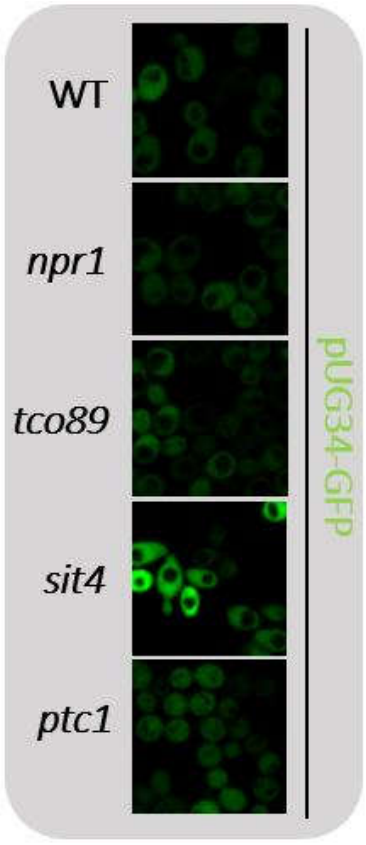

Figure 4.10. Subcellular localization of GFP in the wild-type and set of mutant strains. Images obtained by confocal microscopy of the expression of GFP in the wild-type and set of mutant strains if the BY4741 genetic background. The strains were cotransformed with the pUG34-GFP and the PRS411 plasmids and grown on SD medium to exponential phase. Representative images are shown.

In order to complete our analysis of the activity of Npr1 in membrane trafficking as a function of its phosphorylation state, we analyzed the localization of Npr1 on the different mutant strains. For this experiment the set of BY4741 mutants and a wild-type strain were co-transformed with the pUG34-GFP-*NPR1* plasmid, as indicated in the previous section, or with the empty pUG34-GFP vector together with the pRS411 (*MET25*) plasmid and observed by confocal microscopy. For technical reasons, the strains were co-transformed with the plasmid pRS411, which complements the methionine auxotrophy of the BY4741 strain and allows for the induction of the genes in the pUG34GFP plasmid. The cultures were grown to exponential phase and analyzed. Both the phenotype and genotype of the strains was verified and the expression of the proteins was confirmed by western blot (Figure 4.13)(Annex Figures 1 and 2).

Visualization of pUG34-GFP

We first used the strains transformed with GFP to perform a morphological characterization of the strains, and as an expression control for the confocal microscopy analysis.

It was possible to identify a unique morphology of the *sit4* mutant, which was recurrent throughout the confocal microscopy experiments. The cells possess a more elongated shape (Figure 4.10). Apart from that, the only observable difference between the different strains was the vacuolar size and number. The *tco89* strain presented fewer and larger vacuoles and *ptc1* cells presented a larger number of smaller vacuoles.

Visualization of Npr1-GFP

Based on the current model of Npr1 function, we hypothesized that the dephosphorylated, active form of Npr1 would be associated to the plasma membrane, as is observed upon rapamycin treatment. We would also predict that in strains unable to dephosphorylate Npr1 (*sit4* and *ptc1*) we would not observe the rapamycin-dependent re-localization of Npr1. As observed in Figure 4.11, no apparent differences were appreciable between the confocal microscopy images, as all of the images showed only cytosolic signal. The quantification of the internal and PM associated fluorescence was discarded based on this fact and in the low fluorescence level. The morphology of the strains was consistent with the previous experiment with the strains expressing GFP alone.

Moreover, a lag in growth in these strains was observed compared to the others not over-expressing Npr1. This fact was observed in previous experiments carried out in our laboratory using a growth profile assay in the genetic background THY.AP4, where it was concluded that the over expression of Npr1 was toxic (Sirozh, 2015). This explained why the levels of fluorescence in this experiment were lower than in the other confocal microscopy analysis. We have presented here images of each of the strains. However, in the case of *tco89* and *ptc1*, the transformants were extremely difficult to work with and they presented a high degree of variability. In fact, of 12 transformants tested, only one *ptc1* mutant showed detectable expression of Npr1-GFP. A similar situation was observed for *tco89*.

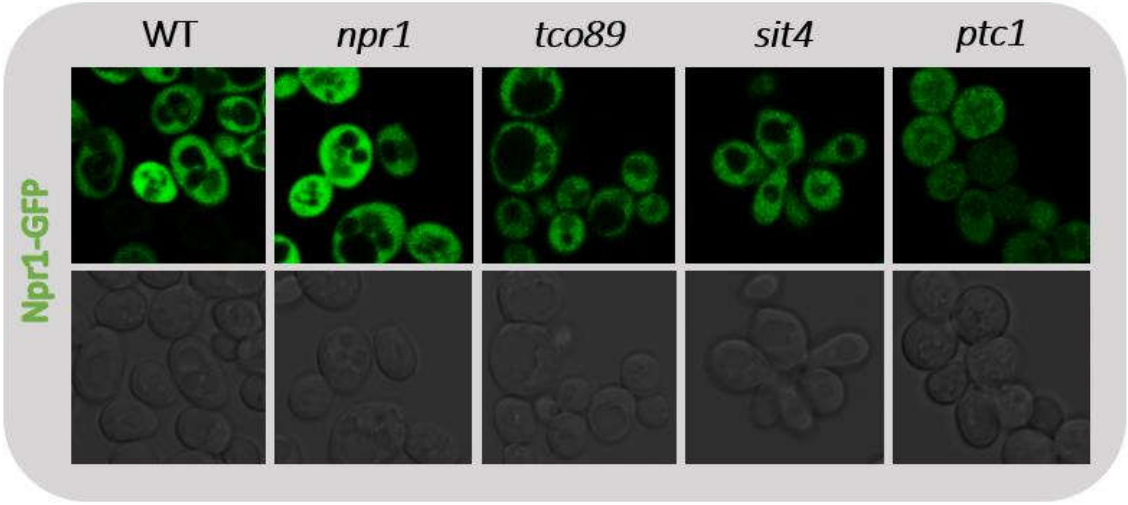

Figure 4.11. Subcellular localization of Npr1-GFP in the wild-type and set of mutant strains. Images obtained by confocal microscopy of the expression of Npr1-GFP in the wild-type and set of mutant strains of the BY4741 genetic background. The strains were co-transformed with the pUG34-GFP-*NPR1* and the pRS411 plasmids and grown on SD medium to exponential phase. Representative images are shown in each case. The experiment was repeated for two clones, obtaining the same results.

Effect of rapamycin on the subcellular localization of Npr1

The results obtained in the previous experiment were expected to be compared to the localization of Npr1-GFP after a rapamycin treatment to the cells. Published reports indicate that the cytosolic subcellular localization of Npr1 is changed to the PM with the addition of rapamycin (MacGurn et al. 2011). It was expected that both in the wild-type and *npr1* mutant, the rapamycin-induced activated Npr1 would change its location to the PM for its transitory interaction with Art1, in order to phosphoinhibit this adaptor and down-regulate the endocytic pathway. In this context, the *tco89* mutant would be predicted to already present Npr1-GFP in the PM before the treatment and the phosphatases mutant strains would prevent the activation of Npr1 and thus its mobilization from the cytosol.

Unfortunately, the fact that not all of the cells presented a reasonable amount of fluorescence implied that we could only perform the rapamycin treatments to the Npr1-GFP transformants of the wild-type and the *npr1* and *sit4* mutants (Figure 4.12). In both the WT and *npr1* mutant the localization of Npr1 changed to the PM. It appears that this Npr1 fusion protein accumulated at the cell surface over time, as the fluorescence signal observed at the PM increased from the 30 to the 60 minutes in the WT cells. No observable differences were seen in the *sit4* mutant. We were unable to complete this experiment in the whole set of mutants due to lack of time and the technical difficulties described above regarding Npr1 toxicity.

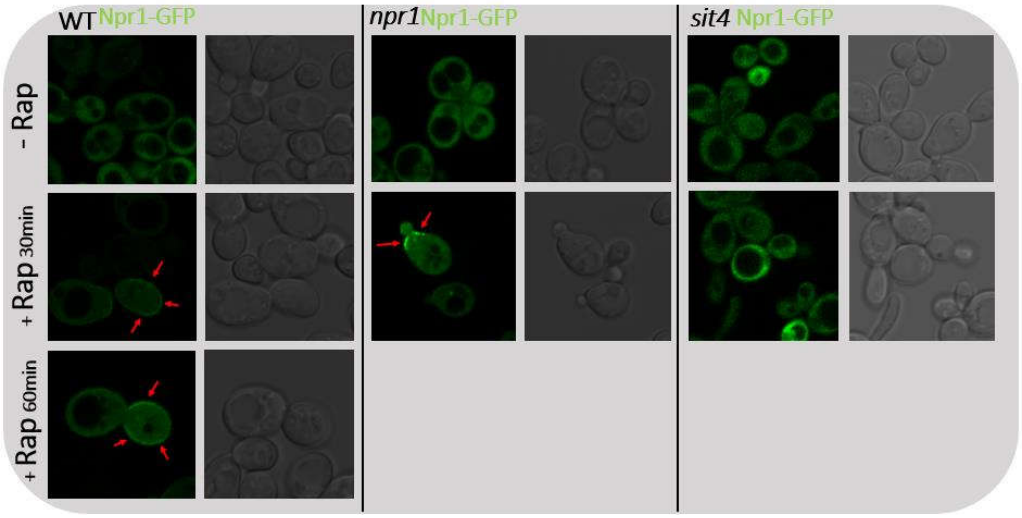

Figure 4.12. Subcellular localization of Npr1-GFP before and after rapamycin treatment. Images obtained by confocal microscopy of the expression of Npr1-GFP in the wild-type and *npr1* strains of the BY4741 genetic background. The strains were cotransformed with the pUG34-GFP-Npr1 and the pRS411 plasmids and grown on SD medium to exponential phase. The cultures were treated for 30min and 60min with rapamycin (200 ng/mL) and visualized by confocal microscopy. Abbreviations: Rapa, rapamycin.

Biochemical study of the phosphorylation state of Npr1 in the mutant strains

The last part of the analysis which was carried out in parallel with the experiments described above was to examine the electrophoretic mobility of Nrp1 in our set of mutants. Upon a rapamycin treatment, Npr1 is known to be dephosphorylated in vivo. It was expected that our set of strains would show steady-state changes in the phosphorylation state of Npr1 and unaltered response to rapamycin, as these mutants lack the proteins that have been proposed to be involved

in the post-translational regulation of Npr1. The phosphorylation state of Npr1 was determined in our set of strains by analyzing the variation of its electrophoretic mobility after a rapamycin treatment. For this purpose, we employed the set of strains described above transformed with the pUG34-GFP-*NPR1* plasmid in which *NPR1* is fused to the green fluorescent protein.

The signals corresponding to the cells untreated with rapamycin indicated the in vivo phosphorylation state of Npr1 in each strain (Figure 4.13). We observed that in the wild-type strain, the major part of Npr1 content was phosphorylated with a small fraction of dephosphorylated, coherent with the fact that Npr1 is constitutively phosphorylated under normal growth conditions, where TORC1 is active. This imbalance in the phosphorylation states was not observed in the *npr1* strain, where both states seemed equivalent. This unexpected difference could be attributed to the higher protein content loaded in the lane, as observed in the higher intensity of the loading control. In any case both strains presented a single band after the rapamycin treatment corresponding to the dephosphorylated state, in accordance with previous reports (Schmidt et al. 1998).

A higher Npr1 content was also observed in *sit4* both in the treated and untreated cells, a fact that has been previously reported (Jacinto et al. 2001). As predicted, in the untreated sample, the electrophoretic mobility of Npr1 was higher than in the wild type control. After the treatment the mobility of the band increased, but Npr1 showed a slower electrophoretic mobility with rapamycin in comparison with the wild-type and *npr1*, indicating a lower degree of dephosphorylation of the protein. The results on *ptc1* were not as encouraging as the ones with *sit4*. Besides the obvious lower expression, the observed phosphorylation shift was comparable to that observed in the wild-type, which indicates that the *ptc1* phosphatase is not necessarily required in the dephosphorylation of Npr1 or that there is a technical problem with the transformant used. This result contradicts earlier reports where, even though a lower-than-normal amounts of Npr1 were reported, a constitutive phosphorylation of Npr1 was observed (González et al. 2009). The reason for this discrepancy is unclear, but could be due to the different media used or a technical issue, such as mutant reversion. As mentioned above, these transformants grew very slowly and this may explain the observed differences. Additional experiments will be required to clarify this issue.

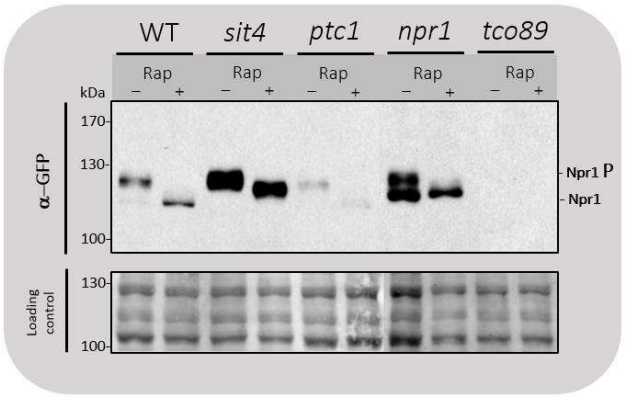

Unfortunately the *tco89* strain presented levels of Npr1-GFP expression below the threshold of detection of the immunoblot, even though some expression was detected in the confocal analysis of one of the transformants (Results shown in the previous section, Figure 4.11). In this case, we were unable to identify the expected single dephosphorylated state of Npr1 without rapamycin treatment.

Figure 4.13. Western blot analysis of the electrophoretic mobility of Npr1 in the mutant strains with (+) and without (-) rapamycin. The wild-type and the indicated mutant strains and of the BY4741 background were cotransformed with the pUG34-GFP-Npr1 and the pRS411 plasmids and grown to exponential phase in SD medium. Half of the culture for each strain was treated 30 minutes with rapamycin (200 ng/mL). The TCA method was used for the extraction of the total protein content of the (+) treated and (-) untreated cultures. Samples were run on a 6% SDS-PAGE gel and the transfer and immunodetection were performed as described in Materials and Methods. The molecular weight markers appear on the left side of the figure (kDa). The Direct Blue staining of the membranes is shown as a loading control. The band corresponding to the phosphorylated Npr1 is indicated as Npr1 P and the dephosphorylated as Npr1 on the right side of the figure.

Discussion

The TORC1 signaling pathway is a central controller of cell growth. It responds to various cellular and environmental cues through diverse effector branches that regulate a broad spectrum of biological processes (Loewith and Hall 2011). Among them, this complex plays the main role in coordinating the cellular response to changes in nitrogen source and availability. The regulation of nitrogen utilization in yeast by TORC1 complex occurs partly through its role in the traffic of membrane transporters mediated by the Npr1 kinase. A large number of studies have focused on this level of regulation, with a well-documented mechanism that involves the ubiquitylation of the target cargo by the Rsp5 E3 ubiquitin ligase for its endocytosis and the function of diverse adaptor proteins, mainly from the ART family (Lauwers et al. 2010).

Despite the amount of individual information for the proteins involved, there is still lack of a consensus regarding the integrative mechanism between the TORC1 response to environmental cues and the membrane trafficking events. In this project we attempted to further explore a published global model of the regulation of endocytosis of nutrient transporters by the TORC1 signaling pathway (MacGurn et al. 2011).

Npr1/Art3 form a complex when Npr1 is inactive

In the study cited above, the Emr group also proposed that other ART proteins could be regulated in the same manner as Art1. By performing a phosphoprofiling experiment, only Art2 and Art3 were detected as being phosphorylated in an Npr1-dependent manner. Art3 was previously reported to work as an adaptor for the ubiquitylation and endocytosis of the aspartic acid transporter Dip5 (Hatakeyama et al. 2010). The case of Art3 is interesting as it establishes a physical interaction with Npr1 (O'Donnell et al. 2010, MacGurn et al. 2011). This fact has not been reported for any other ART protein, and thus could indicate another function of Art3, besides its role as an adaptor.

This interaction was identified in our laboratory to be mediated by the N-terminal arrestin domain of Art3 and the N-terminal regulatory domain of Npr1 (Sirozh, 2015). Despite the fact that this interaction was characterized as being very robust by a yeast-two hybrid assay, it was observed that the inhibition of TORC1 by rapamycin caused Art3 and Npr1 to dissociate. In this study this dissociation was confirmed through another yeast two hybrid assay that included different interaction controls of the Rsp5-mediated endocytic pathway. As expected, the Art3-Rsp5 interaction did not break with rapamycin, which indicated that this compound had a very specific effect for the Art3-Npr1 interaction. This fact along with the observed decrease in Npr1 toxicity with the co-expression of Art3 indicates that the role of Art3 is highly linked to Npr1 functionality.

The function of Npr1 as a TORC1 effector is controlled negatively through phosphorylation (Schmidt et al. 1998). The fact that the inhibition of the TORC1 signaling with rapamycin brought about the dissociation of Art3 and Npr1 implies that the active function of Npr1 is not dependent on Art3. Upon TORC1 signaling the phosphorylated Npr1 forms a complex with Art3 and remains inactive in the cytosol, whereas its dephosphorylation (induced by rapamycin-induced TORC1

inhibition) is incompatible with binding to Art3 and Npr1 is therefore released and changes its subcellular localization to the PM to inhibit Art1-dependent endocytosis (Figure 5.1).

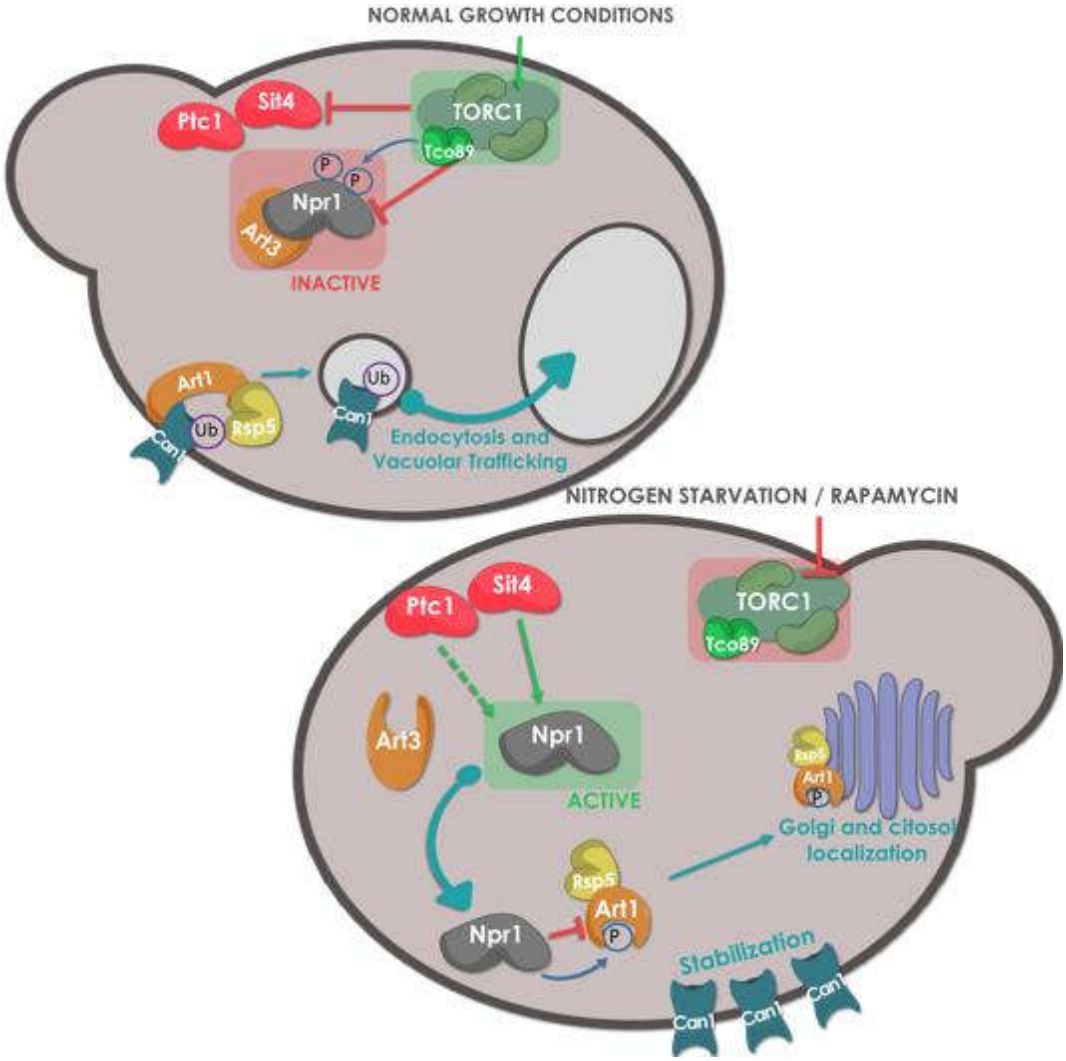

Figure 5.1. Functional implications of the phosphorylation state of the Npr1 TORC1 effector in the regulation of endocytosis. Under normal growth conditions, TORC1 signaling is active and Npr1 is constitutively phosphoinhibited in a Tco89-dependent manner forming a complex with Art3 in the cytosol. This state promotes the endocytosis and vacuolar trafficking of the specific membrane permeases. With the inhibition of TORC1 signaling, as in nitrogen starvation and rapamycin treatment, Npr1 gets dephosphorylated directly by Sit4 and indirectly by Ptc1 and the association with Art3 is broken. The active Npr1 is translocated to the membrane in order to phosphorylate its substrate Art1 and thus stop the endocytic machinery. In this case Can1 is stabilized in the PM and the Rsp5-Art1 complex is degraded.

Effects of the phosphorylation state of Npr1 on membrane trafficking

Hereafter, we discuss the results obtained in our set of experiments carried out with the mutant strains with a described fixed phosphorylation state of Npr1.

- Npr1

The purpose of studying this mutation was to observe the different phenotypes in the absence of endogenous Npr1. The *npr1* mutant strain presented the highest growth rate of all the strains, even more accelerated than the wild type strain. The mutation of *NRP1* under normal conditions

confers a benefit for the cell growth. As described, we also confirmed that this mutant is markedly resistant to rapamycin.

Based on the model of Npr1 function, a similar behavior was expected for the mutants that lack Npr1 activity (*npr1, sit4,* and *ptc1*) regarding its role in the endocytic down-regulation of amino acid permeases. Npr1 presented the expected high resistance to canavanine, as well as AzC, consistent with the down-regulation of the respective permeases. This result seems logical, as the absence of Npr1 would impede the phosphoinhibition of Art1, thus leading to its activation and the subsequent ubiquitylation and degradation of these PM proteins. However, these results are contrasted by the quantification of the Can1-GFP fusion protein present in the plasma membrane. A lower amount of Can1 was expected in comparison with the wild type, but no significant difference was observed in the western blot analysis. The reason for this discrepancy is unclear, but it indicates that the interpretation of the rest of the experiment must be made with caution.

- Tco89

The prediction for this mutant strain was the hypophosphorylated state of Npr1, as it is postulated to mediate Npr1 substrate recognition by TORC1 (Crapeau et al. 2014). In this context, Npr1 would be constitutively active and continually phosphoinhibiting Art1. These cells would have a diminished Rsp5-mediated endocytosis, as the adaptor protein would not be operative. This strain was sensitive to both toxic analogues of proline and arginine, implying a higher amount of these transporters in the PM. Unexpectedly, when the levels of the arginine permease Can1 were measured through confocal microscopy, after transformation with Can1-GFP, no significant differences were found with the wild-type strain. These experiments gave contradictory results to the hypothesis. However, as described above, this analysis may not be conclusive on its own. In any case, it must also be taken into account that Can1 is not the only arginine transporter, as this amino acid (and canavanine) can be introduced through Gap1, the general amino acid permease, and the putative arginine permease Alp1 (Ljungdahl and Daignan-Fornier 2012). Recent results showed that the correct amount of all three arginine permeases is essential for the correct regulation of arginine uptake (Zhang et al. 2016). Gap1 is also known to be stabilized in the membrane by Npr1, thus enhanced Npr1 activity would increase the amounts of Gap1 as well in the membrane, increasing its sensitivity to canavanine.

The *tco89* [*NPR1*-GFP] transformed strain generated considerable technical difficulties, obtaining a very low transformation rate together with low expression of the Npr1-GFP protein, as observed in its fluorescence levels in the confocal microscopy and undetectable protein levels in the western blot assay. In this mutant, Npr1 should be hypophosphorylated, and therefore constitutively active. We have shown previously and in this work that overexpression of Npr1 slows down cell growth, presumably due to toxicity. Therefore, the behavior of the *tco89* mutant overexpressing Npr1 is consistent with an exacerbation of Nrp1 toxicity due to its state of hypophosphorylation leading to hyperactivation. Unfortunately, a dephosphorylated Npr1 band in Figure 4.13 would have tremendously contributed to our hypothesis and the interpretation of the fluorescence images would have been more reliable. Therefore, results on *tco89* are not conclusive and further analysis should be performed.

- Ptc1

The first thing observed for the phosphatases was its inconsistent phenotype in rapamycin. While the other phosphatase mutant, *sit4*, showed rapamycin resistance, *ptc1* was very sensitive to this compound. This would imply a function of this gene in rapamycin tolerance.

The *ptc1* strain presented sensitivity to both toxic amino acid analogues, although in canavanine the strain was able to grow after 6 days. This late growth result was only seen in one of the four biological replicas and so it unlikely to represent a robust phenotype.

The strain presented considerable difficulties to transform and two types of colonies were obtained in all the transformations, varying in their size and growth rate. The smaller colonies presented higher level of expression of the plasmids, so they were used preferentially over the bigger ones. The results obtained for the confocal microscopy images of the Can1-GFP fusion protein were inconclusive, as the bigger colonies presented variable phenotypes and the levels of fluorescence of the smaller colonies were lower than the detectable threshold and the quantification was impossible.

The analysis of the subcellular localization of Npr1 also failed, as from 12 clones analyzed, only one presented fluorescence. We concluded that Npr1 cannot be overexpressed in the *ptc1* mutant strain, due to unknown reasons. What was surprising was that the analysis of the electrophoretic mobility of Npr1 in the *ptc1* mutant did not show an inability to dephosphorylate Npr1 upon rapamycin treatment, which is contradictory to previously reported results (González et al. 2009). We believe that this mutant presents pleiotropic phenotypes which markedly compromise the growth of this strain, therefore leading to difficulties in the genetic manipulation and analysis of transformants.

- Sit4

In this case, disruption of the *SIT4* phosphatase gene is proposed to lead to a reduction in Npr1 activity through hyperphosphorylation. This disruption generates a strain which again presented a decreased growth rate.

In this context, a higher resistance to both toxic analogues was predicted, as under these circumstances Npr1 should not be dephosphorylated in a Sit4-dependent manner and its degree of phosphorylation would be higher than in the wild-type. The case of Sit4 is highly relevant as it is the only mutant showing a phenotype in canavanine coherent with the amount of Can1 present in the PM. Interestingly, the results obtained were the complete opposite to the hypothesized behavior based on the model of Npr1 function. In the predicted model, the less active Npr1 would increase Art1 activity, which is predicted to lead to an increased level of endocytosis of the permeases, thus reducing the amount in the PM and decreasing the effect of canavanine. Not only did this strain exhibit practically equal sensitivity to canavanine as the hypersensitive *tco89*, but the ratio of Can1-GFP found in the PM were significantly higher than the ones in the wild type strain.

As for the subcellular localization of Npr1, our preliminary data indicates that in this strain it was cytosolic as with all of the strains. The only appreciable feature was the reduced expression of the

fusion protein observed by western blot. When treated with rapamycin, the cells did not show a change in subcellular localization of Npr1, as would be expected from the model. In comparison to the Can1 results, the levels of Npr1-GFP fusion protein expression were enhanced in this mutant, as seen in the western blot. The study of the electrophoretic mobility of Npr1 demonstrated that, in fact, the *sit4* mutation does limit the dephosphorylation of Npr1, even though its electrophoretic mobility increases upon treatment, it does not arrive to the dephosphorylated state observed in the wild type control.

The results obtained with the *sit4* mutant are the most interesting. We were able to show a differential amount of the Can1 localization in this strain, explaining its sensitivity to canavanine. The expected results were completely opposite to what was obtained, but indicate an important, and until now, unexpected role of Sit4 in endocytosis. We are not aware of any published data indicating a role of Sit4 in endocytosis. This phosphatase has been described to regulate the intracellular distribution of COPII coat subunits, having a principal role in their dephosphorylation which is required for recycling. It has been shown that the loss of Sit4 disrupts traffic from the ER to the Golgi complex (Bhandari et al., 2013). This important role in the traffic of clathrin-coated vesicles at this level gives us a hint as to the probable role of Sit4 in the regulation of Can1, as clathrin is also known to be a key player in endocytosis (Seto, Bellen and Lloyd 2002).

The results of this project demonstrate an unexpected complexity in the study of the role of Npr1 as an endocytic regulator using the selected approach. The different mutant strains presented a myriad of technical difficulties, especially upon overexpression of Npr1, which lead to severe toxicities impeding the proper interpretation of the experiments in many cases. However, even with all of these difficulties, we were able to generate an important observation: The novel role of the Sit4 phosphatase in the endocytosis of Can1. As described, the disruption of this gene hampered the elimination of this permease from the plasma membrane, causing severe toxicity to canavanine. This result is likely to be independent of Sit4's role in Npr1 regulation and may be related to its more recently described function in regulating components of COPII, as discussed above. Thus, the current project has opened up a new line of investigation that may lead to further insight into the role of the Sit4 phosphatase in vesicle trafficking.

Conclusions

The conclusions obtained in this project are as follows:

1. Art3 and Npr1 from a complex that is dependent on TORC1 signaling as TORC1-inhibition with rapamycin induces the dissociation of the complex. Most likely the dephosphorylation of Npr1 is the cause of the destabilization.

2. *ART3* overexpression attenuates the *NPR1*-mediated toxicity in the presence of rapamycin. The active function of Npr1 is not dependent on Art3, but it might have a role on Npr1 inactivity.

3. The selected approach of using a kinase subunit and phosphatase mutants to study the phosphorylation-dependent function of Npr1 proved to be more complex than expected, likely due to the pleiotropic phenotypes of the mutants chosen. The process of endocytosis is subjected to different types of mechanisms that could be masking our results. The *sit4* and *ptc1* strains presented markedly decreased cell growth, likely reflecting their many cellular functions.

4. The overexpression of *NPR1* in the *tco89* strain was highly toxic. This could be an indicative of the cell's inability to inactivate the in itself toxic Npr1 overexpression by phosphorylation. This phenomenon limited our ability to carry out the proposed analysis.

5. The *ptc1* mutant strain has a pleiotropic phenotype and its indirect effect on Npr1 might be affected by a range of unknown factors. Moreover, an Npr1 phosphorylation shift was observed with rapamycin, contradicting previously reported results. However, *NPR1* overexpression resulted in a strain with very compromised growth, which complicated the interpretation of our analysis.

6. The data presented here suggest a novel role for the Sit4 phosphatase in the endocytosis of the Can1 amino acid permease. All of our obtained results suggest a very deficient Can1 endocytic process in *sit4,* indicating that this phosphatase may play an essential role, not only in ER—Golgi trafficking, but also in the endocytosis of clathrin-coated vesicles. Thus, the current study has opened a new line of investigation which may add to our knowledge regarding the signal transduction pathways involved in regulated endocytosis and the function of the Sit4 phosphatase.

References

ANDRE, B. (1995) An overview of membrane transport proteins in Saccharomyces cerevisiae. *Yeast,* 11**,** 1575-611.

BARBET, N. C., U. SCHNEIDER, S. B. HELLIWELL, I. STANSFIELD, M. F. TUITE & M. N. HALL (1996) TOR controls translation initiation and early G1 progression in yeast. *Mol Biol Cell,* 7**,** 25-42.

BECUWE, M., A. HERRADOR, R. HAGUENAUER-TSAPIS, O. VINCENT & S. LÉON (2012) Ubiquitin-mediated regulation of endocytosis by proteins of the arrestin family. *Biochem Res Int,* 2012**,** 242764.

BONENFANT, D., T. SCHMELZLE, E. JACINTO, J. L. CRESPO, T. MINI, M. N. HALL & P. JENOE (2003) Quantitation of changes in protein phosphorylation: a simple method based on stable isotope labeling and mass spectrometry. *Proc Natl Acad Sci U S A,* 100**,** 880-5.

BREITKREUTZ, A., H. CHOI, J. R. SHAROM, L. BOUCHER, V. NEDUVA, B. LARSEN, Z. Y. LIN, B. J. BREITKREUTZ, C. STARK, G. LIU, J. AHN, D. DEWAR-DARCH, T. REGULY, X. TANG, R. ALMEIDA, Z. S. QIN, T. PAWSON, A. C. GINGRAS, A. I. NESVIZHSKII & M. TYERS (2010) A global protein kinase and phosphatase interaction network in yeast. *Science,* 328**,** 1043-6.

BROACH, J. R. (2012) Nutritional control of growth and development in yeast. *Genetics,* 192**,** 73-105.

CHOI, J., J. CHEN, S. L. SCHREIBER & J. CLARDY (1996) Structure of the FKBP12-rapamycin complex interacting with the binding domain of human FRAP. *Science,* 273**,** 239-42.

CONIBEAR, E. (2010) Converging views of endocytosis in yeast and mammals. *Curr Opin Cell Biol,* 22**,** 513-8.

CRAPEAU, M., A. MERHI & B. ANDRÉ (2014) Stress conditions promote yeast Gap1 permease ubiquitylation and down-regulation via the arrestin-like Bul and Aly proteins. *J Biol Chem,* 289**,** 22103-16.

CRESPO, J. L. & M. N. HALL (2002) Elucidating TOR signaling and rapamycin action: lessons from Saccharomyces cerevisiae. *Microbiol Mol Biol Rev,* 66**,** 579-91, table of contents.

DE CRAENE, J. O., O. SOETENS & B. ANDRE (2001) The Npr1 kinase controls biosynthetic and endocytic sorting of the yeast Gap1 permease. *Journal of Biological Chemistry,* 276**,** 43939-43948.

DE VIRGILIO, C. & R. LOEWITH (2006) Cell growth control: little eukaryotes make big contributions. *Oncogene,* 25**,** 6392-415.

DI COMO, C. J. & K. T. ARNDT (1996) Nutrients, via the Tor proteins, stimulate the association of Tap42 with type 2A phosphatases. *Genes Dev,* 10**,** 1904-16.

EGNER, R. & K. KUCHLER (1996) The yeast multidrug transporter Pdr5 of the plasma membrane is ubiquitinated prior to endocytosis and degradation in the vacuole. *FEBS Lett,* 378**,** 177-81.

FEYDER, S., J. O. DE CRAENE, S. BÄR, D. L. BERTAZZI & S. FRIANT (2015) Membrane Trafficking in the Yeast Saccharomyces cerevisiae Model. *Int J Mol Sci,* 16**,** 1509-1525.

GANDER, S., D. BONENFANT, P. ALTERMATT, D. E. MARTIN, S. HAURI, S. MOES, M. N. HALL & P. JENOE (2008) Identification of the rapamycin-sensitive phosphorylation sites within the Ser/Thr-rich domain of the yeast Npr1 protein kinase. *Rapid Commun Mass Spectrom,* 22**,** 3743-53.

GANDER, S., D. MARTIN, S. HAURI, S. MOES, G. POLETTO, M. A. PAGANO, O. MARIN, F. MEGGIO & P. JENOE (2009) A modified KESTREL search reveals a basophilic substrate consensus for the Saccharomyces cerevisiae Npr1 protein kinase. *J Proteome Res,* 8**,** 5305-16.

GONZÁLEZ, A., A. RUIZ, A. CASAMAYOR & J. ARIÑO (2009) Normal function of the yeast TOR pathway requires the type 2C protein phosphatase Ptc1. *Mol Cell Biol,* 29**,** 2876-88.

GRENSON, M. & E. DUBOIS (1982) Pleiotropic deficiency in nitrogen-uptake systems and derepression of nitrogen-catabolic enzymes in npr-1 mutants of Saccharomyces cerevisiae. *Eur J Biochem,* 121**,** 643-7.

GROSSMANN, G., J. MALINSKY, W. STAHLSCHMIDT, M. LOIBL, I. WEIG-MECKL, W. B. FROMMER, M. OPEKAROVÁ & W. TANNER (2008) Plasma membrane microdomains regulate turnover of transport proteins in yeast. *J Cell Biol,* 183**,** 1075-88.

HAGUENAUER-TSAPIS, R. & ANDRÉ, B. (2004) Membrane trafficking of yeast transporters: mechanisms and physiological control of downregulation. Molecular Mechanisms Controlling Transmembrane Transport. Topics in current genetics, 9:273-323.

HALL, M. N. (1996) The TOR signalling pathway and growth control in yeast. *Biochem Soc Trans,* 24**,** 234-9.

HATAKEYAMA, R., M. KAMIYA, T. TAKAHARA & T. MAEDA (2010) Endocytosis of the aspartic acid/glutamic acid transporter Dip5 is triggered by substrate-dependent recruitment of the Rsp5 ubiquitin ligase via the arrestin-like protein Aly2. *Mol Cell Biol,* 30**,** 5598-607.

HEITMAN, J., N. R. MOVVA & M. N. HALL (1991) Targets for cell cycle arrest by the immunosuppressant rapamycin in yeast. *Science,* 253**,** 905-9.

HELLIWELL, S. B., I. HOWALD, N. BARBET & M. N. HALL (1998) TOR2 is part of two related signaling pathways coordinating cell growth in Saccharomyces cerevisiae. *Genetics,* 148**,** 99-112.

HELLIWELL, S. B., P. WAGNER, J. KUNZ, M. DEUTER-REINHARD, R. HENRIQUEZ & M. N. HALL (1994) TOR1 and TOR2 are structurally and functionally similar but not identical phosphatidylinositol kinase homologues in yeast. *Mol Biol Cell,* 5**,** 105-18.

HICKE, L. (1997) Ubiquitin-dependent internalization and down-regulation of plasma membrane proteins. *FASEB J,* 11**,** 1215-26.

HICKE, L., H. L. SCHUBERT & C. P. HILL (2005) Ubiquitin-binding domains. *Nat Rev Mol Cell Biol,* 6**,** 610-21.

HUGHES HALLETT, J. E., X. LUO & A. P. CAPALDI (2014) State transitions in the TORC1 signaling pathway and information processing in Saccharomyces cerevisiae. *Genetics,* 198**,** 773-86.

HUNTER, T. & G. D. PLOWMAN (1997) The protein kinases of budding yeast: six score and more. *Trends Biochem Sci,* 22**,** 18-22.

JACINTO, E., B. GUO, K. T. ARNDT, T. SCHMELZLE & M. N. HALL (2001) TIP41 interacts with TAP42 and negatively regulates the TOR signaling pathway. *Mol Cell,* 8**,** 1017-26.

JUND, R., E. WEBER & M. R. CHEVALLIER (1988) Primary structure of the uracil transport protein of Saccharomyces cerevisiae. *Eur J Biochem,* 171**,** 417-24.

KATZMANN, D. J., G. ODORIZZI & S. D. EMR (2002) Receptor downregulation and multivesicular-body sorting. *Nat Rev Mol Cell Biol,* 3**,** 893-905.

KEITH, C. T. & S. L. SCHREIBER (1995) PIK-related kinases: DNA repair, recombination, and cell cycle checkpoints. *Science,* 270**,** 50-1.

KOMANDER, D. (2009) The emerging complexity of protein ubiquitination. *Biochem Soc Trans,* 37**,** 937-53.

KOMANDER, D., M. J. CLAGUE & S. URBÉ (2009) Breaking the chains: structure and function of the deubiquitinases. *Nat Rev Mol Cell Biol,* 10**,** 550-63.

KSCHISCHO, M., J. RAMOS & H. SYCHROVÁ (2016) Membrane Transport in Yeast, An Introduction. *Adv Exp Med Biol,* 892**,** 1-10.

KUEPFER, L., M. PETER, U. SAUER & J. STELLING (2007) Ensemble modeling for analysis of cell signaling dynamics. *Nat Biotechnol,* 25**,** 1001-6.

KUNZ, J., R. HENRIQUEZ, U. SCHNEIDER, M. DEUTER-REINHARD, N. R. MOVVA & M. N. HALL (1993) Target of rapamycin in yeast, TOR2, is an essential phosphatidylinositol kinase homolog required for G1 progression. *Cell,* 73**,** 585-96.

KUNZ, J., U. SCHNEIDER, I. HOWALD, A. SCHMIDT & M. N. HALL (2000) HEAT repeats mediate plasma membrane localization of Tor2p in yeast. *J Biol Chem,* 275**,** 37011-20.

KÖLLING, R. & C. P. HOLLENBERG (1994) The ABC-transporter Ste6 accumulates in the plasma membrane in a ubiquitinated form in endocytosis mutants. *EMBO J,* 13**,** 3261-71.

LAUWERS, E., Z. ERPAPAZOGLOU, R. HAGUENAUER-TSAPIS & B. ANDRE (2010) The ubiquitin code of yeast permease trafficking. *Trends in Cell Biology,* 20**,** 196-204.

LEFKOWITZ, R. J., K. RAJAGOPAL & E. J. WHALEN (2006) New roles for beta-arrestins in cell signaling: not just for seven-transmembrane receptors. *Mol Cell,* 24**,** 643-52.

LIN, C. H., J. A. MACGURN, T. CHU, C. J. STEFAN & S. D. EMR (2008) Arrestin-related ubiquitin-ligase adaptors regulate endocytosis and protein turnover at the cell surface. *Cell,* 135**,** 714-25.

LJUNGDAHL, P. O. & B. DAIGNAN-FORNIER (2012) Regulation of Amino Acid, Nucleotide, and Phosphate Metabolism in Saccharomyces cerevisiae. *Genetics,* 190**,** 885-929.

LOEWITH, R. & M. N. HALL (2011) Target of rapamycin (TOR) in nutrient signaling and growth control. *Genetics,* 189**,** 1177-201.

LOEWITH, R., E. JACINTO, S. WULLSCHLEGER, A. LORBERG, J. L. CRESPO, D. BONENFANT, W. OPPLIGER, P. JENOE & M. N. HALL (2002) Two TOR complexes, only one of which is rapamycin sensitive, have distinct roles in cell growth control. *Mol Cell,* 10**,** 457-68.

LORENZ, M. C. & J. HEITMAN (1995) TOR mutations confer rapamycin resistance by preventing interaction with FKBP12-rapamycin. *J Biol Chem,* 270**,** 27531-7.

MACGURN, J. A., P.-C. HSU & S. D. EMR (2012) Ubiquitin and Membrane Protein Turnover: From Cradle to Grave. *Annual Review of Biochemistry, Vol 81,* 81**,** 231-259.

MACGURN, J. A., P. C. HSU, M. B. SMOLKA & S. D. EMR (2011) TORC1 regulates endocytosis via Npr1-mediated phosphoinhibition of a ubiquitin ligase adaptor. *Cell,* 147**,** 1104-17.

MERHI, A. & B. ANDRÉ (2012) Internal amino acids promote Gap1 permease ubiquitylation via TORC1/Npr1/14-3-3-dependent control of the Bul arrestin-like adaptors. *Mol Cell Biol,* 32**,** 4510-22.

METZGER, M. B., V. A. HRISTOVA & A. M. WEISSMAN (2012) HECT and RING finger families of E3 ubiquitin ligases at a glance. *J Cell Sci,* 125**,** 531-7.

NIKKO, E., J. A. SULLIVAN & H. R. B. PELHAM (2008) Arrestin-like proteins mediate ubiquitination and endocytosis of the yeast metal transporter Smf1. *Embo Reports,* 9**,** 1216-1221.

O'DONNELL, A. F., A. APFFEL, R. G. GARDNER & M. S. CYERT (2010) Alpha-arrestins Aly1 and Aly2 regulate intracellular trafficking in response to nutrient signaling. *Mol Biol Cell,* 21**,** 3552-66.

OBRDLIK, EL-BAKKOURY, HAMACHER, CAPPELLARO, VILARINO, FLEISCHER, ELLERBROK, KAMUZINZI & LEDENT (2004) K+ channel interactions detected by a genetic system optimized for systematic studies of membrane protein interactions. *PNAS*.

PICKART, C. M. (2001) Mechanisms underlying ubiquitination. *Annu Rev Biochem,* 70**,** 503-33.

POLAK, A. & M. GRENSON (1973) Evidence for a common transport system for cytosine, adenine and hypoxanthine in Saccharomyces cerevisiae and Candida albicans. *Eur J Biochem,* 32**,** 276-82.

POLO, S. & P. P. DI FIORE (2008) Finding the right partner: science or ART? *Cell,* 135**,** 590-2.

RAVID, T. & M. HOCHSTRASSER (2008) Diversity of degradation signals in the ubiquitin-proteasome system. *Nat Rev Mol Cell Biol,* 9**,** 679-90.

ROTIN, D., O. STAUB & R. HAGUENAUER-TSAPIS (2000) Ubiquitination and endocytosis of plasma membrane proteins: role of Nedd4/Rsp5p family of ubiquitin-protein ligases. *J Membr Biol,* 176**,** 1-17.

SCHMELZLE, T. & M. N. HALL (2000) TOR, a central controller of cell growth. *Cell,* 103**,** 253-62.

SCHMIDT, A., T. BECK, A. KOLLER, J. KUNZ & M. N. HALL (1998) The TOR nutrient signalling pathway phosphorylates NPR1 and inhibits turnover of the tryptophan permease. *EMBO J,* 17**,** 6924-31.

SETO, E. S., H. J. BELLEN & T. E. LLOYD (2002) When cell biology meets development: endocytic regulation of signaling pathways. *Genes Dev,* 16**,** 1314-36.

SHIMOBAYASHI, M., W. OPPLIGER, S. MOES, P. JENÖ & M. N. HALL (2013) TORC1-regulated protein kinase Npr1 phosphorylates Orm to stimulate complex sphingolipid synthesis. *Mol Biol Cell,* 24**,** 870-81.

SIROZH, O. (2015) Characterization of the protein-protein interaction between an alpha-arrestin and its regulatory kinase in *Saccharomyces cerevisiae*

TATE, J. J. & T. G. COOPER (2013) Five conditions commonly used to down-regulate tor complex 1 generate different physiological situations exhibiting distinct requirements and outcomes. *J Biol Chem,* 288**,** 27243-62.

URBAN, J., A. SOULARD, A. HUBER, S. LIPPMAN, D. MUKHOPADHYAY, O. DELOCHE, V. WANKE, D. ANRATHER, G. AMMERER, H. RIEZMAN, J. R. BROACH, C. DE VIRGILIO, M. N. HALL & R. LOEWITH (2007) Sch9 is a major target of TORC1 in Saccharomyces cerevisiae. *Mol Cell,* 26**,** 663-74.

VAN BELLE, D. & B. ANDRÉ (2001) A genomic view of yeast membrane transporters. *Curr Opin Cell Biol,* 13**,** 389-98.

VAN DER REST, M. E., A. H. KAMMINGA, A. NAKANO, Y. ANRAKU, B. POOLMAN & W. N. KONINGS (1995) The plasma membrane of Saccharomyces cerevisiae: structure, function, and biogenesis. *Microbiol Rev,* 59**,** 304-22.

VANDENBOL, M., J. C. JAUNIAUX & M. GRENSON (1990) The Saccharomyces cerevisiae NPR1 gene required for the activity of ammonia-sensitive amino acid permeases encodes a protein kinase homologue. *Mol Gen Genet,* 222**,** 393-9.

VANDENBOL, M., J. C. JAUNIAUX, S. VISSERS & M. GRENSON (1987) Isolation of the NPR1 gene responsible for the reactivation of ammonia-sensitive amino-acid permeases in Saccharomyces cerevisiae. RNA analysis and gene dosage effects. *Eur J Biochem,* 164**,** 607-12.

WEI, Y. & X. F. ZHENG (2011) Nutritional control of cell growth via TOR signaling in budding yeast. *Methods Mol Biol,* 759**,** 307-19.

WULLSCHLEGER, S., R. LOEWITH & M. N. HALL (2006) TOR signaling in growth and metabolism. *Cell,* 124**,** 471-84.

WULLSCHLEGER, S., R. LOEWITH, W. OPPLIGER & M. N. HALL (2005) Molecular organization of target of rapamycin complex 2. *J Biol Chem,* 280**,** 30697-704.

ZAMAN, S., S. I. LIPPMAN, X. ZHAO & J. R. BROACH (2008) How Saccharomyces responds to nutrients. *Annu Rev Genet,* 42**,** 27-81.

ZHANG, P., G. DU, H. ZOU, J. CHEN, G. XIE, Z. SHI & J. ZHOU (2016) Effects of three permeases on arginine utilization in Saccharomyces cerevisiae. *Sci Rep,* 6**,** 20910.

Annex

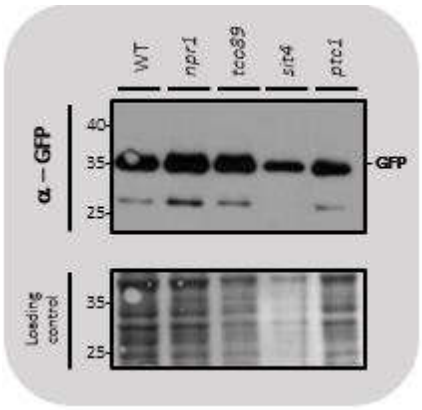

Figure 1. Western blot analysis of pUG34-GFP expression levels. The indicated strains were transformed with the pUG34GFP plasmid and grown to exponential phase in SD medium. The TCA method was used for the extraction of the total protein content. Samples were run on an 8% SDS-PAGE gel and the transfer and immunodetection were performed as described in Materials & Methods. The molecular weight markers appear on the left side of the figure (kDa). The Direct Blue staining of the membrane is shown as a loading control.

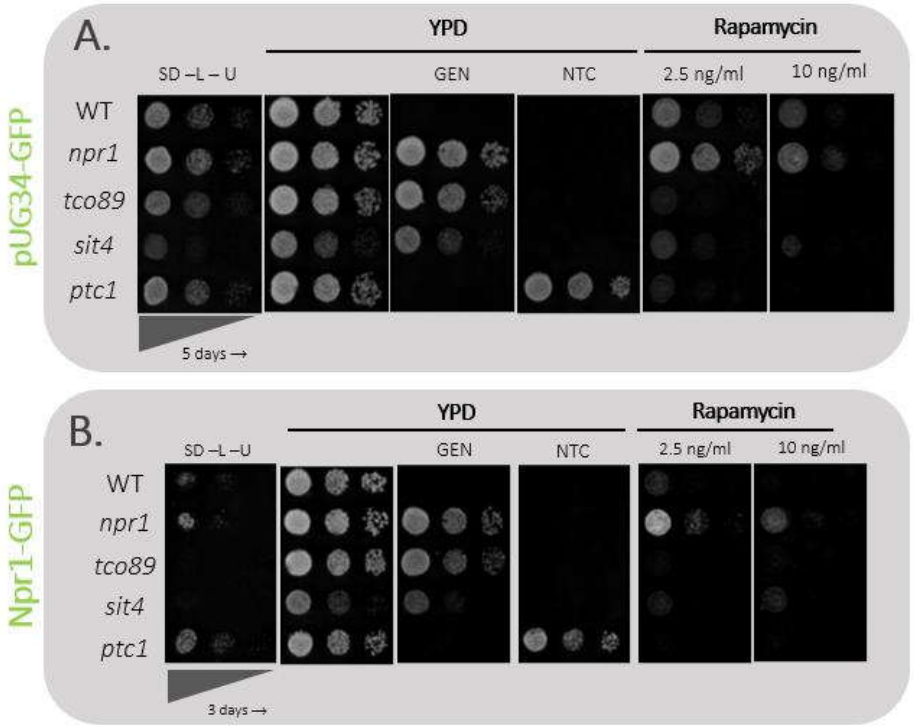

Figure 2. pUG34-GFP and Npr1-GFP transformants verification drop tests. The resulting transformants were grown to saturation in SD –L –U and, after serial dilutions, drops were placed on solid plates with the compounds indicated in the figure. Both genotypic and phenotypic growth tests in rapamycin were performed. Two clones were analyzed with same results. Abbreviations: GEN, geneticin; NTC; nourseothricin.